

ESCAPE

Preparing Forecasting Systems for the Next generation of Supercomputers

Batch 2: **Definition of novel** Weather & **Climate Dwarfs**

Dissemination Level: Public

This project has received funding from the European Union's Horizon 2020 research and innovation programme under grant agreement No 67162





























Energy-efficient Scalable Algorithms for Weather Prediction at Exascale

Author Andreas Mueller, Mike Gillard, Kristian Pagh Nielsen, Zbigniew Piotrowski

Date 07/12/2017

Research and Innovation Action H2020-FETHPC-2014

Project Coordinator: Dr. Peter Bauer (ECMWF)

Project Start Date: 01/10/2015
Project Duration: 36 month

Published by the ESCAPE Consortium

Version: 1.1

Contractual Delivery Date: 31/12/2017

Work Package/ Task: WP1/T1.1

Document Owner: ECMWF

Contributors: ECMWF, LU, PSNC, DMI

Status: Final

Contents

1	Execu	tive summary
2	Introd	uction
	2.1	Background
	2.2	Scope of this deliverable
3	Descri	ption of individual Dwarfs
	3.1	Multigrid preconditioned elliptic solver
		MPDATA for unstructured meshes
	3.3	MPDATA for structured meshes
	3.4	ACRANEB2 radiation scheme
4	Concli	usions 48

1 Executive summary

This deliverable contains the description of the characteristics of a second set of so-called numerical weather & climate prediction dwarfs that form key functional components of prediction models in terms of the science that they encapsulate and in terms of computational cost they impose on the forecast production. The ESCAPE work flow between work packages centres on these dwarfs and hence their selection, their performance assessment, code adaptation and optimisation is crucial for the success of the project. These new dwarfs have been chosen with the purpose of extending the range of computational characteristic represented by the dwarfs previously selected in batch 1 (see Deliverable D1.1). The dwarfs have been made, their documentation has been compiled and the software has been made available on the software exchange platform.

The dwarfs in this deliverable include a multigrid elliptic solver, a novel advection scheme for unstructured meshes, an advection scheme for structured meshes and a radiation scheme. This deliverable includes their scientific description and the guidance for installation, execution and testing. This documentation is equivalent to the one available from the ESCAPE Confluence web-page that disseminates the project outcomes.

2 Introduction

2.1 Background

ESCAPE stands for Energy-efficient Scalable Algorithms for Weather Prediction at Exascale. The project develops world-class, extreme-scale computing capabilities for European operational numerical weather prediction and future climate models. ESCAPE addresses the ETP4HPC Strategic Research Agenda 'Energy and resiliency' priority topic, promoting a holistic understanding of energy-efficiency for extreme-scale applications using heterogeneous architectures, accelerators and special compute units by:

- Defining and encapsulating the fundamental algorithmic building blocks underlying weather and climate computing;
- Combining cutting-edge research on algorithm development for use in extreme-scale, high-performance computing applications, minimising time- and cost-to-solution;
- Synthesising the complementary skills of leading weather forecasting consortia, university research, high-performance computing centres, and innovative hardware companies.

ESCAPE is funded by the European Commission's Horizon 2020 funding framework under the Future and Emerging Technologies - High-Performance Computing call for research and innovation actions issued in 2014.

2.2 Scope of this deliverable

2.2.1 Objectives of this deliverable

This document accompanies the prototype implementations of the second batch of weather and climate dwarfs developed in WP1. The dwarfs are used by WPs 2, 3, and 4 for code adaptation, hybrid computing and benchmarking and diagnostics. The document aims to provide a documentation of the provided dwarfs to ensure that they are easily usable by the respective partners. The dwarf implementations are available at: https://git.ecmwf.int/projects/ESCAPE.

2.2.2 Work performed in this deliverable

As per the task description in the Description of Action for task 1.1, the work performed in this deliverable included the isolation and packaging of a second set of canonical NWP algorithms and internal model workflows, including:

- Multigrid elliptic solver (dwarf-D-ellipticSolver-GCR-multigrid, see Section 3.1)
- MPDATA for unstructured meshes (dwarf-D-advection-MPDATA, see Section 3.2)
- MPDATA for structured meshes (dwarf-D-advection-MPDATA-structured, see Section 3.3)
- ACRANEB2 radiation scheme (dwarf-P-radiation-ACRANEB2, see Section 3.4)

2.2.3 Deviations and counter measures

Deviations and counter measures were not required for the completion of this deliverable.

3 Description of individual Dwarfs

This section contains the description of the dwarfs presented in this deliverable including instructions to install and run them. References are listed at the end of each subsection.

3.1 Multigrid preconditioned elliptic solver

3.1.1 Scope

Bespoke scalable, preconditioned non-symmetric elliptic solvers are one of key areas of investigations aimed at forming Weather & Climate dwarfs. They are commonly employed within compressible or sound-proof atmospheric models that use semi-implicit schemes permitting large time-steps. Consequently they form an important element required to provide robust solution procedures for NWP applications. However effective preconditioning strategies suitable for their efficient exploitation and their scalability properties need to be explored further.

Dwarf-D-ellipticSolver-GCR-multigrid implements the Generalised Conjugate Residual (GCR) method and utilises a bespoke multigrid preconditioner. It is adopted in conjunction with compact stencil schemes, based on the finite volume method, that can prove to be an attractive option for next generation HPC facilities given their reduced communication costs (due to their intrinsic data locality).

The multigrid preconditioning provides one of the potential options aiming at devising a procedure reducing time to solution for NWP. The three-dimensional potential-flow problem constitutes a suitable benchmark for experimenting with different preconditioners to evaluate their competitiveness, especially in terms of number of iterations required to reach convergence and scalability.

3.1.2 Objectives

The main objectives of this dwarf are to improve the computational time per iteration of the GCR algorithm and to reduce the number of iterations to convergence. These two aspects are crucial, since a consistent reduction of the computational cost might allow GCR algorithms, in conjunction with compact finite-volume discretisation, to become very competitive for NWP applications. A well preconditioned, robust elliptic solver embedded in a semi-implicit time discretization that allows large time-steps provides an attractive procedure for next-generation HPC infrastructures.

The evaluation of this dwarf will focus on the use of multigrid techniques as part of operator preconditioning within the elliptic solver.

3.1.3 Definition

Dwarf-D-ellipticSolver-GCR-multigrid delivers an implementation that involves the solution of linear elliptic equations through the GCR method [1, 2, 3] using a Finite Volume (FV) discretisation in space. It solves a three-dimensional elliptic problem, namely a potential flow past a Gaussian-shaped hill on the sphere. In the following, we first describe the GCR method for a general linear elliptic problem – including an exploration of the relevant preconditioning approaches available.

3.1.3.1 Generalized Conjugate-Residual approach

In this section we follow closely section 5 of [3]. In particular, we can formulate the GCR approach starting from the following linear elliptic problem:

$$\mathcal{L}(\varphi) = R$$
 where $\mathcal{L}(\varphi) = \sum_{I=1}^{3} \frac{\partial}{\partial x^{I}} \left(\sum_{J=1}^{3} C^{IJ} \frac{\partial \varphi}{\partial x^{J}} + D^{I} \right) - A\varphi,$ (1)

where A, C^{IJ} , D^I , R are variable coefficients which for the proposed test case would account for metric coefficients related to the use of geophysical coordinates in a global model. In our implementation we use periodic boundary conditions to ensure flow continuity on a sphere and Neumann boundary conditions at the top (atmosphere) and bottom (orography) of the computational domain. The discrete representation of a field is denoted by the subscript i such that the discrete linear operator is represented by \mathcal{L}_i while the inner product by $\langle \xi, \zeta \rangle = \sum_i \xi_i \zeta_i$.

The GCR approach utilises operator preconditioning, where the preconditioning operator, \mathcal{P} , is a linear operator that approximates \mathcal{L} . In fact, \mathcal{P} can be any operator such that $\mathcal{L}\mathcal{P}^{-1}$ is negative definite, but to be effective as part of the elliptic solver it should both approximate \mathcal{L} and be easier to invert than \mathcal{L} . This leads to the revised problem:

$$\frac{\partial \mathcal{P}(\varphi)}{\partial \tau} = \mathcal{L}(\varphi) - R. \tag{2}$$

Eq. 1 is then substituted by the auxiliary problem, $\mathcal{P}^{-1}[\mathcal{L}(\varphi) - R] = 0$.

The GCR method can then be obtained through variational arguments (see for instance [2, 3]). As such, our auxiliary problem (Eq. 2) is generalised to a kth-order damped oscillation equation:

$$\frac{\partial^{k} \mathcal{P}(\varphi)}{\partial \tau^{k}} + \frac{1}{T_{k-1}(\tau)} \frac{\partial^{k-1} \mathcal{P}(\varphi)}{\partial \tau^{k-1}} + \dots + \frac{1}{T_{1}(\tau)} \frac{\partial \mathcal{P}(\varphi)}{\partial \tau} = \mathcal{L}(\varphi) - R, \tag{3}$$

that is discretized in pseudo-time τ . This forms the affine discrete equation for the progression of the residual errors r. The optimal parameters $T_1, ..., T_{k-1}$ are identified and an integration increment, $\Delta \tau$, is chosen to ensure that the minimization of the residual errors in the norm defined by the inner product $\langle r, r \rangle$, is successful.

This leads to the following algorithm:

Algorithm 1 Generalized Conjugate Residual, GCR(k), method

For any initial guess, φ_i^0 , set $r_i^0 = \mathcal{L}(\varphi_i^0) - \mathcal{R}_i$, $p_i^0 = \mathcal{P}^{-1}(r_i^0)$; then iterate:

For
$$n = 1, 2, ...$$
 until convergence

for
$$v = 0, ..., k - 1$$

$$\beta = \frac{\langle r^{\nu} \mathcal{L}(p^{\nu}) \rangle}{\langle \mathcal{L}(p^{\nu}) \mathcal{L}(p^{\nu}) \rangle},$$

$$\varphi_i^{\nu+1} = \varphi_i^{\nu} + \beta p_i^{\nu},$$

$$r_i^{\nu+1} = r_i^{\nu} + \beta \mathcal{L}_i(p^{\nu}),$$
exit if $||r_i^{\nu+1}|| \le \epsilon$,
$$e_i = \mathcal{P}_i^{-1}(r^{\nu+1}),$$
evaluate $\mathcal{L}_i(e) = \left[\sum_{l=1}^3 \frac{\partial}{\partial x^l} \left(\sum_{J=1}^3 C^{IJ} \frac{\partial \varphi}{\partial x^J} + D^I\right) - A\varphi\right],$
for $l = 0, ...\nu$

$$\alpha_l = \frac{\langle \mathcal{L}(e)\mathcal{L}(p^l) \rangle}{\langle \mathcal{L}(p^l)\mathcal{L}(p^l) \rangle},$$

$$p_i^{\nu+1} = e_i + \sum_l \alpha_l p_i^l,$$

$$\mathcal{L}_i(p^{\nu+1}) = \mathcal{L}_i(e) + \sum_l \alpha_l \mathcal{L}_i(e^l),$$
reset $[\varphi, r, e, \mathcal{L}(e)]_i^k$ to $[\varphi, r, e, \mathcal{L}(e)]_i^0$

Here, n and ν represent the external iteration of the solver and internal iteration of orders of the damped oscillator respectively. The output of the preconditioner, ℓ represents an approximation of the error in ℓ associated with the residual equation. The quality of this approximation depends heavily on the choice of ℓ , where consideration is also given to how quickly ℓ can be inverted. A detailed description of this can be found in the following section.

3.1.3.2 Operator preconditioning for GCR

As detailed in the previous section, large time-step semi-implicit integrators within compressible or sound-proof atmospheric models depend on complex non-symmetric elliptic solvers. The condition number of the underlying sparse linear operator is $O(10^{10})$, which necessitates bespoke operator preconditioning. The primary source of stiffness in the elliptic solver, due to the choice of discretization, is in the vertical. Due to the geometrically thin shell that represents the atmosphere of a global system, the resolution in atmospheric depth is significantly higher than any current operational horizontal resolution. This stiffness is restrictive enough to cause the elliptic solver to have great difficulty converging when solving for global systems.

A practical choice to address the vertical stiffness is to utilise effective preconditioning. The choice of $\mathcal P$ and how it is inverted can have a dramatic effect on the convergence rate of the elliptic solver. We choose a deflation [3] type method, which has two stages. Firstly, we take a $\mathcal P \approx \mathcal L$, such that the off diagonal $(I \neq J)$ contributions to Eq. 1 are discarded; (this will be true of all choices of $\mathcal P$). The second stage is to split $\mathcal P$ into two parts, the vertical part (I = 3) and horizontal part (I = 1, 2). If the vertical component is treated implicitly, while the horizontal part is treated explicitly, the operator inversion becomes a two-step process. The first step evolves the explicit horizontal component using Richardson-type iteration [3], which in turn provides a source term for what is now a straightforward tri-diagonal problem. This tridiagonal system can be solved using a bespoke form of a well-known algorithm (Thomas algorithm [5]). The preconditioned component of Algorithm 1 is defined as follows:

$$e = \mathcal{P}^{-1}(r)$$
, where $r = \mathcal{L}(\varphi) - \mathcal{R}$ (4)

Take $\mathcal{P} \approx \mathcal{L}$, such that,

$$\mathcal{P} = \sum_{I=1}^{3} \frac{\partial}{\partial x^{I}} \left(C^{II} \frac{\partial \varphi}{\partial x^{I}} + D^{I} \right) - A\varphi \tag{5}$$

In this application, our general elliptic problem (Eq. 5) takes the form detailed in [2] and is set out in the test case section – where D and A are zero, C becomes a product of a vector, scalar and a tensor, and the whole thing is normalised so as to give our residual error the sense of being a dimensionless velocity on the grid.

Now, split $\mathcal{P} = \mathcal{P}_V + \mathcal{P}_H$, treating the horizontal component explicitly and the vertical component implicitly:

$$\frac{\partial \varphi}{\partial \tilde{\tau}} = \mathcal{P}(e) - r,\tag{6}$$

$$\frac{\varphi^{\mu+1} - \varphi^{\mu}}{\Delta \tilde{\tau}} = \mathcal{P}_V \left(\varphi^{\mu+1} \right) + \mathcal{P}_H \left(\varphi^{\mu} \right) - r, \tag{7}$$

$$(I - \Delta \tilde{\tau} \mathcal{P}_V) \varphi^{\mu+1} = \varphi^{\mu} + \Delta \tilde{\tau} \left(\mathcal{P}_H(\varphi^{\mu}) - r \right) \equiv R. \tag{8}$$

So,

$$\varphi^{\mu+1} = (I - \Delta \tilde{\tau} \mathcal{P}_V)^{-1} R. \tag{9}$$

Although Eq. 9 is formally pentadiagonal, a simple adaptation of the Thomas algorithm can be used to invert the remaining operator. This approach inverts the horizontal part of $\mathcal P$ approximately if Eq. 8, 9 are cycled for a few iterations in pseudo-time $\tilde{\tau}$. The inversion of the vertical operator is obtained using a direct solver. The iterative parameter $\Delta \tilde{\tau}$ is only limited by the spectral properties of $\mathcal P_H$, and so can be much larger than that of a Richardson iteration in $\mathcal P$, which would be limited by the aforementioned vertical anisotropy. Although the Thomas algorithm is inherently serial in the vertical component, the structure of the

underlying domain decomposition of our global meshes avoids any massively parallel issues as the vertical towers at any given mesh node are contiguous in memory. The inability to locally thread the algorithm is compensated by the speed and simplicity of the Thomas algorithm. This approach is used when multigrid is turned off, and time-step splitting is turned off.

A similar approach to the above deflation preconditioner (Eq. 8, 9) can be used, whereby the vertical inversion is split into two half time-step parts, one before the horizontal evolution and one after. The steps are detailed as follows:

$$\varphi^{\mu + \frac{1}{2}} = \varphi^{\mu} + \frac{\Delta \tilde{\tau}}{2} \left(\mathcal{P}_V \left(\varphi^{\mu + \frac{1}{2}} \right) - r \right), \tag{10}$$

$$\varphi^* = \varphi^{\mu + \frac{1}{2}} + \Delta \tilde{\tau} \mathcal{P}_H \left(\varphi^{\mu + \frac{1}{2}} \right), \tag{11}$$

$$\varphi^{\mu+1} = \varphi^* + \frac{\Delta \tilde{\tau}}{2} \left(\mathcal{P}_V \left(\varphi^{\mu+1} \right) - r \right). \tag{12}$$

This approach can also be expanded, by evolving the horizontal step (Eq. 11) through a larger number of iterations. The total half time step inversions of Eq. 10 and 12 will then be half of the total pseudo-time evolved while iterating Eq. 11. We will utilise this property by applying a multigrid v-cycle solver for the horizontal evolution (Eq. 11), which will allow for a much greater pseudo time-step to be utilised during the vertical inversion step. It will also allow for the vertical inversion to occur twice, firstly to initialise the first guess of solution error used by the horizontal evolution step and secondly to finalise the solution error before returning to the elliptic solver – ensuring that the critical vertical direction has been resolved by the preconditioner.

3.1.3.3 Operator preconditioning with Multigrid

Given the two deflation solvers above, it is possible to consider utilising multigrid techniques to improve the capability of the iterative approximation for the horizontal inversion. Discrete iterative techniques are often quick to reduce errors with oscillatory frequencies that are well captured on the discrete grid resolution and within the operator stencil utilised by the technique. They do not address errors with higher frequency than can be easily resolved by the underlying grid, or lower frequencies not captured well on the stencil. The model on its own will not be able to capture and resolve details associated with the former, higher frequency errors. However, the lower frequency errors can be reduced only when discretisations can represent those frequencies adequately.

Multigrid can be used to alter the discretisation as it allows iterative techniques to be applied to the same problem, over a range of different resolutions. Specifically, a multigrid v-cycle approach can be used to systematically link the iterative processes occurring at each resolution by solving a hierarchy of residual error problems on a set of nested meshes. For a given grid level, an auxiliary residual problem is solved on the coarser grid level, which will return the coarse grid error correction to be added to the solution on the current grid level. The same type of iterative methods can be used at each grid level, including the coarsest level –

alternatively a more involved direct solve may be employed at the coarsest grid level (where the computational cost will be vastly reduce) and simpler iterative processes can be used at intermediate grid levels, with the main task of smoothing the residual errors associated with their grid resolution. These smoothing processes can be performed both before and after the coarse grid errors have been evolved. This is the 'v' in the v-cycle, where iterative processes smooth solution errors for increasing grid resolution, then coarse grid corrections are applied as the grid resolution reduces back towards the finest grid level.

Details of coarse grid generation and restriction and prolongation methods for nested multigrid hierarchies on the octahedral mesh can be found in D1.5.

The following pseudo-code details the v-cycle algorithm:

Algorithm 2 Recursive multigrid v-cycle

Recursive multigrid algorithm:

```
Initialise solution error if required.
```

```
Multigrid_Vcycle(e, r) for input solution error and residual.
```

```
if ( on coarsest level ) Solve( e , r ) \rightarrow move back to next finer mesh.

else

Presmooth ( e , r ).

calculate new residual:

rr = \mathcal{P}(e) - r.

Restrict to next coarse mesh level:

rr \Rightarrow rr_c and set ee, ee_c = 0.

call recursion \rightarrow move to next coarser mesh level:

Multigrid_Vcycle( ee_c , rr_c ).

Prolong coarse mesh error:

ee_c \Rightarrow ee.

adjust current mesh level solution error by coarse mesh

e = e + ee.
```

error:

e = e + ee. Postsmooth (e, r). \rightarrow move to next finer grid level.

exit multigrid v-cycle when finest grid level reached.

Finalise solution error if required, before returning to elliptic solver.

Algorithm 2 details the general steps of a multigrid v-cycle. On all grids with higher resolution than the coarsest grid, an iterative solver is applied to smooth the solution error associated with the current grid resolution. After smoothing, a new residual problem is formulated and restricted to the next coarsest grid level. Upon reaching the coarsest grid level, a smoother/solver is applied to the current grid residual error problem. This coarse grid correction is then returned to the next finest grid level, whereby the coarse grid residual error is added to the solution error at the current grid level. The corrected solution may then undergo a further pass of the iterative smoother, in such situations where the coarse grid correction is likely to reintroduce errors removed by the previous iterative evolution of solution error at this grid level. This coarse grid correction to the next finer grid repeats until the finest grid level is reached. This method also allows for the solution to be initialized and finalized if desired. Outside of the initialization step, a first guess of the solution error associated with a particular grid level is taken to be zero.

Various advanced forms of this approach, e.g. W-cycle can be utilized, but they are likely to be too costly to be used in a preconditioner. The improvement in solution error provided by

the preconditioner can easily come at higher computational expense than when the error is reduced by the GCR elliptic solver iterations instead. Therefore, effective preconditioning needs to balance between accuracy of the error correction and computational cost to arrive at that correction. The relative importance of the vertical anisotropy and efficiency of the vertical inversion compared to the much lower horizontal anisotropy at resolutions currently in operation makes extra computational investment in improving the horizontal inversion difficult to recover.

This dwarf (dwarf-D-ellipticSolver-GCR-multigrid) implements a multigrid v-cycle to the split time-step detailed in Eq. 10-12. The solution is initialized by first inverting in the vertical for a total of half the total pseudo time-step evolution to be applied during evolution of Eq. 11. A Richardson iterative solver is used for all horizontal smoothing and solving steps; where the pseudo time-step, $\Delta \tilde{\tau} \equiv \beta_H$, for a given resolution is derived from a spectral evaluation of \mathcal{P}_H on the finest grid level. Each coarsening step roughly doubles the resolution in each horizontal direction, so a $2\Delta \tilde{\tau}$ time-step is permissible on a coarser mesh. As the resolution of the dual mesh for a given grid is somewhat variable, a pseudo time-step derivation can also be conducted for each grid individually.

The action of Algorithm 2 on Eq. 11 leads to an evolution on the finest grid level, set $\varphi' = \varphi^{\mu + \frac{1}{2}}$, then iterate:

$$\varphi^* = \varphi' + \beta_H \mathcal{P}_H(\varphi') , \quad \varphi' = \varphi^*. \tag{13}$$

Given the solution φ^* on the finest grid level, evaluate the residual error associated with this solution,

$$\mathcal{P}(\varphi^*) = r$$
, restrict $r \to r_c$, and set $e_c = 0$. (14)

Here, A_c indicates values restricted to the next coarsest grid level. Therefore, a solution to the residual problem:

$$\mathcal{P}_H(e_c) = r_c, \tag{15}$$

can be used to modify the current solution to Eq. 13 to provide better estimate of the actual solution, $\tilde{\varphi}^* \approx \varphi^* - e$, where $e_c \to e$, such that the coarse grid correction error is prolonged back to the finer grid.

Further coarse grid corrections act on the residual problem arising from Eq. 15,

$$\mathcal{P}_H(e_c) - r_c = rr_c, \quad rr_c \to rr_{c^2}, \quad ee_{c^2} = 0. \tag{16}$$

Here, c^2 refers to the next coarsest grid after level c. rr and ee correspond to the residual of the residual problem in Eq. 15 and the error associated with the solution error is Eq. 15, on the given coarse grid level. The residual problem to solve on grid c^2 is then:

$$\mathcal{P}_H(ee_{c^2}) = rr_{c^2}$$
, where $ee_{c^2} \to ee_c$ and $e_c \to e_c - ee_c$. (17)

The coarse grid error correction on grid c^2 is prolonged back to the next finest grid level c, where the solution error associated with grid c is corrected by the next coarsest grid error associated with grid c^2 . The solution error is then prolonged back to the finest grid, and used to correct the original solution:

$$e_c \to e$$
, $\varphi^* \to \varphi^* - e$. (18)

The solution φ^* then should have had any errors associated with the resolutions of the fine grid and the next two coarsest grid levels removed. This can now be used in Eq. 12 and then passed back to the elliptic solver.

This structure of residual error correction steps can occur for as many coarse grid levels as are generated. For the generation of nested coarse grids for the octahedral mesh, see D1.5 – which also discusses alternative smoother options.

3.1.3.4 Test Case

This dwarf solves the same potential flow problem as dwarf-D-ellipticSolver-GCR, namely potential flow over a Gaussian-shaped hill – governed as follows:

$$v = v_a - \nabla \varphi,$$

$$\nabla \cdot (\rho v) = 0,$$
(19)

where v_a is the ambient velocity and $\rho = \rho(z)$ is the prescribed density.

The above problem seeks a φ that satisfies the set of equations to be solved – thus providing a better initial guess for the given problem, cast in non-orthogonal, terrain following coordinates. The vertical coordinate is adjusted to the mountain profile, depending on the model depth, H, and mountain profile, h(x, y). The terrain following reference frame involves metric terms, introduced via a transformation matrix, G, and its associated Jacobian, G [2].

$$G^{IJ} = \sum_{K=1}^{2} \frac{\partial x^{I}}{\partial x^{K}} \frac{\partial x^{J}}{\partial x^{K}}$$

$$J = \left[\det(G) \right]^{\frac{1}{2}}$$
(20)

Eq. 19 then becomes:

$$u = u_{a} - \frac{\partial \varphi}{\partial x} - G^{13} \frac{\partial \varphi}{\partial z},$$

$$v = v_{a} - \frac{\partial \varphi}{\partial y} - G^{23} \frac{\partial \varphi}{\partial z},$$

$$w = w_{a} - J^{-1} \frac{\partial \varphi}{\partial z},$$

$$\frac{\partial \rho^{*} u}{\partial x} + \frac{\partial \rho^{*} v}{\partial y} + \frac{\partial \rho^{*} w}{\partial z}.$$
(21)

The contravariant velocity, $w = J^{-1}w + G^{13}u + G^{23}v$, and $\rho^* = J\rho$.

The associated boundary conditions are obtained using the pressure force vector P_f , using the contravariant velocity. This leads to the elliptic problem to be solved:

$$-\frac{1}{\rho^*} \nabla \cdot \left(\rho^* \mathbf{P}_f(\varphi, \nabla \varphi) \right) = -\frac{1}{\rho^*} \nabla \cdot \left(\rho^* \left(\mathbf{v}^* - \mathbf{P}_f \right) \right) = 0, \tag{22}$$

with contravariant velocity, $v^* = (u, v, w)$. Eq. 22 is then solved using the multigrid preconditioned GCR(k) elliptic solver in dwarf-D-ellipticSolver-GCR-multigrid. For a detailed derivation and description of this test, see [2].

3.1.3.5 I/O interfaces

This dwarf has a simple input/output (I/O) layout. Specifically, the interfaces in terms of I/O data are as follows:

- **Input**: an Atlas-type field in grid-point space, defined on a Finite-Volume type mesh. This represents the initial guess of the scalar function that is necessary to compute;
- Output: an Atlas-type field in grid-point space, defined on a Finite-Volume type mesh. This represents the converged value of the scalar function we needed to compute.

The dimensions of these Atlas-type fields are determined by the grid employed that can be specified in the input files (.json format). The dwarf utilises octahedral grids, which can be specified in the input files as O#, e.g. O180. For more details on how to run the dwarf, refer to section 3.1.6.

3.1.4 Prototype

The prototype, prototype1, implements the elliptic solver core routines relying on the Atlas data-structure and based on the Fortran90 programming language. The dwarf is divided into a main file and various module files:

- dwarf-D-ellipticSolver-GCR-multigrid-prototype1.F90, which implements the main program;
- dwarf_D_ellipticSolver_GCR_coreLoop.F90, which contains the core loops of the GCR algorithm as reported in algorithm 1;
- dwarf_D_ellipticSolver_GCR_linear_operators_module.F90, which contains the implementation of the linear operator L;
- dwarf_D_ellipticSolver_GCR_initial _module.F90, which contains the initialisation for the model;
- dwarf_D_ellipticSolver_GCR_nabla_operators_module.F90, which contains the implementation of the various 'nabla' operators, such as Gradient, Divergence and Laplacian;
- dwarf_D_ellipticSolver_GCR_preconditioner_module.F90, which contains a trivial preconditioner (this can be modified in order to build an efficient preconditioner);
- dwarf_D_ellipticSolver_GCR_mappings_module.F90, which contains the necessary mappings for using spherical coordinates;
- dwarf_D_ellipticSolver_GCR_topology_module.F90, which defines the surface topography of the problem;
- dwarf_D_ellipticSolver_GCR_auxiliary_module.F90, which contains some support functionalities.
- dwarf_D_ellipticSolver_GCR_multigrid_setup_module.F90, which contains nested mesh generation functionality.
- dwarf_D_ellipticSolver_GCR_multigrid_tools_module.F90, which contains multigrid tools to match and move between nested meshes.

defined in Note that the code algorithm 1 is contained within the file dwarf D ellipticSolver GCR coreLoop.F90, inside the subroutine GCR k. Preconditioning approaches including multigrid routines, are contained dwarf D ellipticSolver GCR preconditioner module.F90. Coarse grid generation, using Atlas, is handled by dwarf D ellipticSolver GCR multigrid setup module.F90 - while general multigrid grid matching, prolongation, and restriction operators can be found in dwarf D ellipticSolver GCR multigrid tools module.F90.

3.1.5 Dwarf installation and testing

In this section we describe how to download and install the dwarf along with all its dependencies, and we show how to run it for a simple test case. Note that dwarf-DelipticSolver-GCR-multigrid is implemented using *Atlas*, the ECMWF software framework that supports flexible data-structures for NWP. Currently, the dwarf is written in Fortran 2003.

3.1.5.1 Download and Installation

The first step is to download and install the dwarf along with all its dependencies. With this purpose, it is possible to use the script provided under the ESCAPE software collaboration platform: https://git.ecmwf.int/projects/ESCAPE.

Here you can find a repository called escape. You need to download it. There are two options to do this. One option is to use ssh. For this option you need to add an ssh key to your bitbucket account at https://git.ecmwf.int/plugins/servlet/ssh/account/keys. The link "SSH keys" on this website gives you instructions on how to generate the ssh key and add them to your account. Once this is done you should first create a folder named, for instance, ESCAPE, enter into it and subsequently download the repository by using the following the steps below:

```
mkdir ESCAPE

cd ESCAPE/
git clone ssh://git@git.ecmwf.int/escape/escape.git
```

The other option to download the repo is by using https instead of ssh. Instead of the git command above you then need to use

```
git clone
https://<username>@git.ecmwf.int/scm/escape/escape.git
```

where <username> needs to be replace by your bitbucket username.

Once the repository is downloaded into the ESCAPE folder just created, you should find a new folder called escape. The folder contains a sub-folder called bin that has the python/bash script (called escape) that needs to be run for downloading and installing the dwarf and its dependencies. To see the various options provided by the script you can type:

```
./escape/bin/escape -h
```

To download the dwarf you need to run the following command:

```
./escape/bin/escape checkout \
dwarf-D-advection-MPDATA-structured --ssh
```

To use https you need to replace --ssh with --user <username>. The commands above automatically check out the develop version of the dwarf. If you want to download a specific branch of this dwarf, you can do so by typing:

```
./escape/bin/escape checkout \
dwarf-D-ellipticSolver-GCR-multigrid -ssh \
--version <branch-name>
```

An analogous approach can be used for the --user version of the command. You should now have a folder called dwarf-D-ellipticSolver-GCR.

In the above command, you can specify several other optional parameters. To see all these options and how to use them you can type the following command:

```
./escape checkout -h
```

At this stage it is possible to install the dwarf and all its dependencies. This can be done in two different ways. The first way is to compile and install each dependency and the dwarf separately:

```
./escape/bin/escape generate-install \
dwarf-D-ellipticSolver-GCR-multigrid
```

The command above will generate a script called install-dwarf-D-ellipticSolver-GCR that can be run by typing:

```
./install-dwarf-D-ellipticSolver-GCR-multigrid
```

This last step will build and install the dwarf along with all its dependencies in the following paths:

```
dwarf-D-ellipticSolver-GCR-multigrid/builds/
dwarf-D-ellipticSolver-GCR-multigrid/install/
```

The second way is to create a bundle that compiles and installs all the dependencies together:

```
./escape/bin/escape generate-bundle \
dwarf-D-ellipticSolver-GCR-multigrid
```

This command will create an infrastructure to avoid compiling the single third-party libraries individually when some modifications are applied locally to one of them. To complete the compilation and installation process, after having run the above command for the bundle, simply follow the instructions on the terminal.

In the commands above that generate the installation file, you can specify several other optional parameters. To see all these options and how to use them you can type the following command:

```
./escape generate-install -h
./escape generate-bundle -h
```

3.1.5.2 Testing

The dwarf should be tested to verify it is working as expected. For this purpose, a testing framework was created that allows for the verification that the main features of the dwarf are working correctly.

Various regression tests are provided for each sub-dwarf in order to allow the results to be consistent when the underlying algorithms are modified, and to test additional features or different hardware. The regression tests can be found in the folder test that is located in each sub-dwarf folder. Scripts running the code on different architectures, e.g. the Cray HPC at ECMWF, are provided for each sub-dwarf in the folder run-scripts located in each sub-dwarf folder.

To run this verification, you should run the following command:

```
ctest -j<number-of-tasks>
```

from inside the builds/dwarf-D-ellipticSolver-GCR-multigrid folder.

Instructions on running the executable are given in the next section

3.1.6 Run the Dwarf

The prototype driver dwarf-D-ellipticSolver-GCR-prototype1, and the corresponding fortran modules, can be modified in dwarf-DellipticSolver-GCR-multigrid/sources/dwarf-D-ellipticSolver-GCR-multigrid/src/prototype1. The protoptype can be built by running

```
make -j<number-of-tasks>
```

From within the dwarf-D-ellipticSolver-GCR-multigrid/builds/dwarf-D-ellipticSolver-GCR-multigrid folder.

The executable should be run from a fresh directory to store any output files using a specified .json file as follows:

```
./dwarf-D-ellipticSolver-GCR-
multigrid/builds/bin/dwarf-D-ellipticSolver-GCR-
prototype1 \
--config /dwarf-D-ellipticSolver-GCR-
multigrid/sources/dwarf-D-ellipticSolver-GCR-
multigrid/src/tests/ dwarf-D-ellipticSolver-GCR-
multigrid-032.json.
```

The performance for the proscribed test case for the various preconditioning options can be evaluated by setting various options within the <u>.json</u> file. An example file is provided: <u>dwarf-D-ellipticSolver-GCR-multigrid-O32.json</u>. For convenience and completeness, a local version of the .json file can be used from within the current working directory.

If the dwarf is to be run on an HPC machine available to the ESCAPE partners, an automatically generate job submission script can be created using the escape file. More specifically, if you run the following command:

```
./escape generate-run -c \
/dwarf-D-ellipticSolver-GCR-
multigrid/builds/bin/dwarf-D-ellipticSolver-GCR-
prototype1 \
--config <path_to_json_file>/<json_file_name>.json
```

This allows the code to generate the submission script for the given HPC machine targeted without submitting the actual job. The command above generates an escape.job file in the current folder. This can successively be submitted via qsub on the HPC.

In the above command other optional parameters can be specified, such as wall-time, number of tasks, number of threads, etc. To view all possible options and how to set them up, use the following command:

```
./escape generate-run -h
```

3.1.7 Integration

This dwarf explores the solution of a linear elliptic operator in spherical coordinates and arises in the context of mesh-based discretizations (such as the finite volume method). In particular, this dwarf can be integrated in a global Weather & Climate model involving a semi-implicit time-stepping scheme and a mesh-based spatial discretization. This, for instance, occurs in the solution of the horizontal part of an NWP model.

Therefore, the key aspects for this dwarf to be integrated within a Weather & Climate model are:

- Mesh-based discretization (e.g. finite-volume or finite-element methods);
- Solution of the 3D elliptic problem arising from the semi-implicit discretization in time where separability of horizontal and vertical coordinates is no longer satisfied (different from the semi-implicit discretization in existing spectral models).

If these three aspects are present in the NWP model, this dwarf can be integrated to solve the horizontal Laplacian of the model in a semi-implicit and mesh-based manner.

3.1.8 References

- [1] S.C. Eisenstat, H.C. Elman, and M.H. Schultz. Variational iterative methods for nonsymmetric systems of linear equations. *SIAM Journal on Numerical Analysis*, 20(2):345–357, 1983.
- [2] P.K. Smolarkiewicz and L.G. Margolin. Variational solver for elliptic problems in atmospheric flows. *Appl. Math. Comp. Sci*, 4(4):527–551, 1994.
- [3] P.K. Smolarkiewicz and L.G. Margolin. Variational methods for elliptic problems in fluid models. In *Proc. ECMWF Workshop on Developments in numerical methods for very high resolution global models*, pages 137–159, 2000.
- [4] P.K. Smolarkiewicz and J.A. Pudykiewicz. A class of semi-Lagrangian approximations for fluids. *J. Atmos. Sci.*, 49:2082–2096, 1992.
- [5] L.H.Thomas. Elliptic problems in linear differential equations over a network. Watson Sci. Comput. Lab Report, Columbia University, New Youk, 1949.

3.2 MPDATA for unstructured meshes

3.2.1 Scope

MPDATA stands for multidimensional positive definite advection transport algorithm. We have two versions of this dwarf: one for structured meshes and one for unstructured meshes. The version for structured meshes is used in the COSMO-EULAG model. Measurements have shown that depending on the number of processors used about 25% to 34% of the entire runtime of the model is spent in the MPDATA dwarf. The unstructured version described in this document is used in a newly developed finite volume dynamical core at ECMWF called FVM. We expect similar importance of this dwarf in FVM like in COSMO-EULAG.

3.2.2 Objectives

As described before the MPDATA algorithm takes a significant amount of the runtime of FVM. For this reason the key objectives of this dwarf are

- the optimisation of the runtime per time-step of the MPDATA algorithm and
- exploration of new hardware architectures like GPUs and Xeon Phi processors to accelerate its computation

The dwarf offers an isolated prototype for advection on the sphere using an unstructured mesh with the MPDATA algorithm to facilitate work on optimising its performance and exploring new processors.

3.2.3 Definition

3.2.3.1 Fundamental concept The fundamental idea behind the MPDATA algorithm can be illustrated for the 1D advection equation of a field $\psi(x,t)$ with a constant advection velocity v > 0:

$$\frac{\partial \psi}{\partial t} + \frac{\partial}{\partial x} (v \, \psi) = 0. \tag{23}$$

The analytical solution of this equation is given by

$$\psi(x,t) = \psi_0(x - vt). \tag{24}$$

with the initial distribution $\psi_0(x) = \psi(x, t_0)$ at some initial time t_0 . To solve (36) numerically we discretise time and space by introducing grid points (nodes) x_i and time steps t_n . The simplest method to solve (36) is the so called upwind scheme in which we approximate the time derivative by a finite difference forward in time and the spatial derivative by a left sided finite difference (for v > 0). This gives us

$$\psi_i^{n+1} = \psi_i^n - \frac{\delta t \, v}{\delta x} (\psi_i^n - \psi_{i-1}^n) \tag{25}$$

To make this scheme more accurate we use Taylor expansion up to second order in δx and δt :

$$\psi_i^{n+1} \approx \psi_i^n + \delta t \frac{\partial \psi}{\partial t} + \frac{1}{2} \delta t^2 \frac{\partial^2 \psi}{\partial t^2}$$
 (26)

$$\psi_{i-1}^n \approx \psi_i^n - \delta x \frac{\partial \psi}{\partial x} + \frac{1}{2} \delta x^2 \frac{\partial^2 \psi}{\partial x^2}$$
 (27)

Introducing these Taylor expansions into the upwind scheme (38) leads to

$$\psi_i^n + \delta t \frac{\partial \psi}{\partial t} + \frac{1}{2} \delta t^2 \frac{\partial^2 \psi}{\partial t^2} = \psi_i^n - \frac{\delta t \, v}{\delta x} \left[\delta x \frac{\partial \psi}{\partial x} - \frac{1}{2} \delta x^2 \frac{\partial^2 \psi}{\partial x^2} \right] \tag{28}$$

We can eliminate the second derivative in time by using the PDE (36):

$$\frac{\partial^2 \psi}{\partial t^2} \stackrel{(36)}{=} -v \frac{\partial^2 \psi}{\partial t \partial x} \stackrel{(36)}{=} v^2 \frac{\partial^2 \psi}{\partial x^2} \tag{29}$$

Using this in (41) and rearranging the terms leads to the following equation

$$\frac{\partial \psi}{\partial t} = -\frac{\partial}{\partial x}(v\,\psi) - \frac{\partial}{\partial x}\left[-\frac{v\,\delta x}{2}\frac{\partial \psi}{\partial x} + \frac{v\,\delta t}{2}\frac{\partial}{\partial x}(v\,\psi)\right]. \tag{30}$$

We can interpret the last term in the square brackets for $\psi \neq 0$ as an anti-diffusive flux. This can be illustrated by defining an anti-diffusive pseudo-velocity $v_{\rm ad}$ which allows to write the equations which MPDATA solves as

$$\frac{\partial \psi}{\partial t} = -\frac{\partial}{\partial x} (v \, \psi) - \frac{\partial}{\partial x} (v_{\text{ad}} \, \psi). \tag{31}$$

$$v_{\rm ad} = -\frac{v \, \delta x}{2\psi} \frac{\partial \psi}{\partial x} + \frac{v \, \delta t}{2\psi} \frac{\partial}{\partial x} (v \, \psi). \tag{32}$$

3.2.3.2 Generalisation for the Sphere The unstructured MPDATA dwarf solves the following more general equation

$$\frac{\partial (G\,\psi)}{\partial t} + \frac{\partial}{\partial x}\,(v\,\psi) = 0,\tag{33}$$

where the symbol G describes geometric and physical terms (Jacobian of coordinate transformations and fluid density) which are also included here in a modified advection velocity v. We use in this dwarf the so called infinite-gauge version of MPDATA which allows the field ψ to change its sign by essentially removing ψ from the denominator in (45). This gives us together with the introduction of G the following expression for the pseudo-velocity $v_{\rm ad}$:

$$v_{\rm ad} = -\frac{1}{2}|v|\frac{\partial \psi}{\partial x}\delta x + \frac{1}{2}v\,\delta t \left[\frac{\partial}{\partial x}(v\,\psi) + \psi\,\frac{\partial G}{\partial t}\right]. \tag{34}$$

Descretising (44) with forward difference in time gives

$$\psi_i^{n+1} = \psi_i^n - \delta t \frac{\partial}{\partial x} (v \, \psi) - \delta t \frac{\partial}{\partial x} (v_{\text{ad}} \, \psi). \tag{35}$$

The spatial derivatives are discretised with upwind fluxes which results in three dimensions in a sum of the upwind fluxes over all interfaces between neighbouring grid cells. The derivation of the multidimensional case and more details about its implementation are described in [1]. A pre-print of this paper can be found in doc/MPDATA-JCP2016.pdf in the git-repo.

3.2.3.3 Implementation To illustrate the implementation of MPDATA we indicate the order of the different functions by the horizontal coloured bars beneath the following two equations. These equations are only meant to be a basic illustration of the code. Differently from these equations the full code is three dimensional.

$$\psi_i^{n+1} = \psi_i^n - \delta t \frac{\partial}{\partial x} (v \, \psi) - \delta t \frac{\partial}{\partial x} (v_{\text{ad}} \, \psi)$$

$$v_{\text{ad}} = -\frac{1}{2} |v| \frac{\partial \psi}{\partial x} \delta x + \frac{1}{2} u \, \delta t \left[\frac{\partial}{\partial x} (v \, \psi) + \psi \, \frac{\partial G}{\partial t} \right]$$

$$0.411$$

The numbers next to each bar stand for one of the functions of the dwarf as given by the following pseudo-code:

main program: loop over all timesteps. In each step:

1. compute_upwind_flux:

for all edges: for all levels: compute the upwind flux for that edge

2. compute upwind fluz:

for all nodes: for all levels: compute the upwind flux between vertically neighbouring grid cells

3. compute_fluxzdiv:

for all nodes: for all levels:

compute sum over all horizontal and vertical fluxes weighted with
the surface of the corresponding face

4. advance solution:

for all nodes: for all levels: add computed sum to the advected field pD multiplied with the timestep and divided through the density

5. rhofac_correction:

for all nodes: for all levels:

compute product of density and advected field

6. compute_centered_flux:

for all edges: for all levels:

compute centred (averaged) flux for that edge

7. compute_centered_fluz:

for all nodes: for all levels:

compute centred flux between vertically neighbouring grid cells

8. compute_fluxzdiv:

for all nodes: for all levels:

compute sum over all horizontal and vertical centred fluxes
weighted with the surface of the corresponding face

9. halo_exchange:

communicate results between neighbouring processors

10. compute_pseudovel_xy:

for all edges: for all levels:
 compute first term in the pseudo-velocity for that edge
for all edges: for all levels:
 compute second term in the pseudo-velocity and add to first term

11. compute_pseudovel_z:

for all nodes: for all levels:

compute first term in the pseudo-velocity between vertically
neighbouring grid cells

for all nodes: for all levels:

compute second term in the pseudo-velocity and add to first term

for vertically neighbouring grid cells

12. limit flux

13. compute fluxzdiv:

for all nodes: for all levels:

compute sum over all horizontal and vertical antidiffusive fluxes

weighted with the surface of the corresponding face

14. advance solution:

for all nodes: for all levels:

add computed sum to the advected field pD multiplied with the
timestep and divided through the density

15. halo exchange:

communicate results between neighbouring processors

3.2.4 Dwarf usage and testing

In this section we describe how to download and install the dwarf along with all its dependencies, and we show how to run it for a simple test case.

Note that the MPDATA dwarf for unstructured meshes is implemented using Atlas, the ECMWF software framework that supports flexible data-structures for NWP. The dwarf is written in Fortran 2003. Extensions to C++ can be envisioned if necessary and they can be implemented using Atlas.

3.2.4.1 Download and installation The first step is to download and install the dwarf along with all its dependencies. With this purpose, it is possible to use the script provided under the ESCAPE software collaboration platform: https://git.ecmwf.int/projects/ESCAPE.

Here you can find a repository called <code>escape</code>. You need to download it. There are two options to do this. One option is to use ssh. For this option you need to add an ssh key to your bitbucket account at https://git.ecmwf.int/plugins/servlet/ssh/account/keys. The link "SSH keys" on this website gives you instructions on how to generate the ssh key and add them to your account. Once this is done you should first create a folder named, for instance, ESCAPE, enter into it and subsequently download the repository by using the following the steps below:

```
mkdir ESCAPE
cd ESCAPE/
git clone ssh://git@git.ecmwf.int/escape/escape.git
```

The other option to download the repo is by using https instead of ssh. Instead of the git command above you then need to use

```
git clone https://<username>@git.ecmwf.int/scm/escape/escape.git
```

where <username> needs to be replace by your bitbucket username.

Once the repository is downloaded into the **ESCAPE** folder just created, you should find a new folder called **escape**. The folder contains a sub-folder called **bin** that has the python/bash script (called **escape**) that needs to be run for downloading and installing

the dwarf and its dependencies. To see the various options provided by the script you can type:

```
./escape/bin/escape -h
```

To download the dwarf you need to run the following command:

```
./escape/bin/escape checkout dwarf-D-advection-MPDATA \
--ssh
```

To use https you need to replace —ssh with —user <username>. The commands above automatically check out the **develop** version of the dwarf. If you want to download a specific branch of this dwarf, you can do so by typing:

```
./escape/bin/escape checkout dwarf-D-advection-MPDATA --user <username> \
--version <branch-name>
```

You should now have a folder called dwarf-D-advection-MPDATA.

At this stage it is possible to install the dwarf and all its dependencies. This can be done in two different ways. The first way is to compile and install each dependency and the dwarf separately:

```
./escape/bin/escape generate-install dwarf-D-advection-MPDATA
```

The command above will generate a script called install-dwarf-D-advection-MPDATA that can be run by typing:

```
./install-dwarf-D-advection-MPDATA
```

This last step will build and install the dwarf along with all its dependencies in the following paths:

```
dwarf-D-advection-MPDATA/builds/
dwarf-D-advection-MPDATA/install/
```

The second way is to create a bundle that compiles and installs all the dependencies together:

```
./escape/bin/escape generate-bundle dwarf-D-advection-MPDATA
```

This command will create an infrastructure to avoid compiling the single third-party libraries individually when some modifications are applied locally to one of them. To complete the compilation and installation process, after having run the above command for the bundle, simply follow the instructions on the terminal.

In the commands above that generate the installation file, you can specify several other optional parameters. To see all these options and how to use them you can type the following command:

```
./escape generate-install -h
./escape generate-bundle -h
```

3.2.4.2 Testing You should now verify that the dwarf works as expected. For this purpose, we created a testing framework that allows us to verify that the main features of the dwarf are working correctly.

In particular, for each sub-dwarf we provide various regression tests in order to allow the results to be consistent when the underlying algorithms are modified, and to test additional features or different hardware. The regression tests can be found in the folder test that is located in each sub-dwarf folder. For each sub-dwarf we also provide scripts running the code on different architectures, e.g. the Cray HPC at ECMWF, that can be found in the folder run-scripts located in each sub-dwarf folder.



Tip

We encourage partners who are testing different architectures to add and/or modify the scripts!

To run this verification, you should run the following command:

```
ctest -j<number-of-tasks>
```

from inside the builds/dwarf-D-advection-MPDATA folder.

Warning



We strongly advise you to verify via ctest that the main functionalities of the dwarf are working properly any time you apply modifications to the code. Updates that do not pass the tests cannot be merged. In addition, if you add a new feature to the dwarf, this should be supported by a test if the existing testing framework is not already able to verify its functionality.

For instructions on how to run the executables see the next section.

Tip



The tests rely on the tolerance specified in the config-files. This tolerance has been chosen in such a way that single and double precision simulations pass the test if the build type is set to Bit. This has been tested successfully at ECMWF with GFortran, Intel (version 16.0.3) and Cray compilers. However, the tests might fail with some compilers (at ECMWF with the Cray compiler) when using build type Release. If tests fail on your platform please make sure that you use build type Bit!

3.2.5 Run the Dwarf

If you want to run the dwarf in your local machine, you could do so by using the executable files inside

```
dwarf-D-advection-MPDATA/install/dwarf-D-advection-MPDATA/bin/
```

In this section we assume that the executable has been generate with the generate-install option of the escape script. If you used the generate-bundle option you should replace <code>install/dwarf-D-advection-MPDATA</code> with <code>builds/bundle/bin</code>.

The executables need the specification of a configuration file. The configuration files can be found at

```
dwarf-D-advection-MPDATA/sources/dwarf-D-advection-MPDATA/config-files/
```

The executable can be run as follows:

```
dwarf-D-advection-MPDATA/install/dwarf-D-advection-MPDATA/\
bin/dwarf_D_advection_MPDATA --config \
dwarf-D-advection-MPDATA-solidBody-pole-032.json
```

where, if the <code>.json</code> file is not in the current directory, you can specify its path after <code>--config</code>. We used <code>dwarf-D-advection-MPDATA-solidBody-pole-032.json</code> in the last command as an example for one of the configuration files. This configuration file contains the parameters for a solid body rotation over the poles. There are also configuration files for a rotation along the equator (<code>dwarf-D-advection-MPDATA-solidBody-equator-032.json</code>) as well as a rotation along a direction in between those two (<code>dwarf-D-advection-MPDATA-solidBody-di</code>. The configuration files write by default output-files every 100 timesteps which can be plotted with <code>gmsh</code> (<code>http://gmsh.info</code>). There are also copies of these configuration files ending with <code>-noOut</code> where the parameter iout is set to 0 which does not create any output. These <code>-noOut</code> configuration files should be used for performance measurements.

If you instead want to run the dwarf on an HPC machine available to the ESCAPE partners, you can automatically generate the job submission script with the **escape** file.

More specifically, if you run the following command:

```
./escape generate-run -c \
"dwarf-D-advection-MPDATA/install/dwarf-D-advection-MPDATA/\
bin/dwarf_D_advection_MPDATA_-config_\
dwarf-D-advection-MPDATA-solidBody-pole-032.json"
```

This allows the code to generate the submission script for the given HPC machine you are targeting without submitting the actual job. The command above will in fact simply generate an <code>escape.job</code> file in the current folder. This can successively be submitted via <code>qsub</code> on the HPC machine you want to run the simulation on.

In the above command you can specify several other optional parameters, such as wall-time, number of tasks, number of threads, etc. To see all these options and how to set them up you can type the following command:

```
./escape generate-run -h
```

The following subsections describe how the precision of the computation can be selected and the data generated by the simulation in the log- and output-files.

3.2.5.1 Switching between single and double precision. The dwarf has been tested with single as well as double precision. The error tolerance in the configuration files has been chosen in such a way that all compilers should pass the test with both single and double precision if build type Bit is used. To switch between single and double precision please adjust the line integer, parameter, public :: wp = sp inside the file dwarf_D_advection_MPDATA_auxiliary_module.F90. Setting wp = dp in this line uses double precision for the entire simulation whereas wp = sp uses single precision.

3.2.5.2 Log and output data

Error measures In each output-step as defined by the parameter **iout** in the configuration file the code measures the accuracy of the result by comparing the numerical result with an analytical result. For better comparison with the literature [2] a number of different error measures are computed:

- EMIN: error of the minimum value of the advected tracer
- EMAX: error of the maximum value of the advected tracer
- ERR0 (L2-error): root-mean-square error of the solution
- ERR1: normalised error of the mean field
- ERR2: variance of the field
- Linf-error: maximum of the error

The most important error measures are the L2- and Linf-error. Only these two are considered when comparing the result with the reference result stored in the configuration file.

Wallclock-time of the timeloop The code uses the Fortran function <code>system_clock</code> to measure the time between starting and finishing the timeloop. This measurement should be used when comparing different computer architectures. For accelerators please also include a measurement that includes the process of copying the data to the device. Please report your measurements (no matter if they are good or bad) on https://confluence.ecmwf.int/display/ESCAPE/Dwarf+-+D+-+advection+-+MPDATA by following the example under the section "Performance Measurements" of that website.

3.2.6 References for unstructured MPDATA

- [1] C. Kühnlein and P.K. Smolarkiewicz. "An unstructured-mesh finite-volume MP-DATA for compressibleatmospheric dynamics". In: *Journal of Computational Physics* (submitted 2016).
- [2] P.K. Smolarkiewicz and P.J. Rasch. "Monotone advection on the sphere: an Eulerian versus semi-Lagrangian approach". In: *Journal of the Atmospheric Sciences* (1990).

3.3 MPDATA for structured meshes

3.3.1 Scope

MPDATA stands for multidimensional positive definite advection transport algorithm. We have two versions of this dwarf: one for structured meshes and one for unstructured meshes. The version for structured meshes described in this document is used in the COSMO-EULAG model for regional NWP. Measurements have shown that depending on the number of processors used about 25% to 34% of the entire runtime of the model is spent in the MPDATA dwarf. The unstructured version is used in a newly developed finite volume dynamical core at ECMWF called FVM. We expect similar importance of this dwarf in FVM like in COSMO-EULAG.

3.3.2 Objectives

Since this dwarf may significant share of the runtime of the weather model (as the number of passive tracers e.g. chemical species grows, the share can be very large), it is important that we optimise it as much as possible and explore the use of GPUs and Xeon Phi processors to accelerate its computation. This is the key objective behind this dwarf.

3.3.3 Definition

3.3.3.1 Fundamental concept The fundamental idea behind the MPDATA algorithm can be illustrated for the 1D advection equation of a field $\psi(x,t)$ with a constant

advection velocity v > 0:

$$\frac{\partial \psi}{\partial t} + \frac{\partial}{\partial x} (v \, \psi) = 0. \tag{36}$$

The analytical solution of this equation is given by

$$\psi(x,t) = \psi_0(x - vt). \tag{37}$$

with the initial distribution $\psi_0(x) = \psi(x, t_0)$ at some initial time t_0 . To solve (36) numerically we discretise time and space by introducing grid points (nodes) x_i and time steps t_n . The simplest method to solve (36) is the so called upwind scheme in which we approximate the time derivative by a finite difference forward in time and the spatial derivative by a left sided finite difference (for v > 0). This gives us

$$\psi_i^{n+1} = \psi_i^n - \frac{\delta t \, v}{\delta x} (\psi_i^n - \psi_{i-1}^n) \tag{38}$$

To make this scheme more accurate we use Taylor expansion up to second order in δx and δt :

$$\psi_i^{n+1} \approx \psi_i^n + \delta t \frac{\partial \psi}{\partial t} + \frac{1}{2} \delta t^2 \frac{\partial^2 \psi}{\partial t^2}$$
(39)

$$\psi_{i-1}^n \approx \psi_i^n - \delta x \frac{\partial \psi}{\partial x} + \frac{1}{2} \delta x^2 \frac{\partial^2 \psi}{\partial x^2}$$
(40)

Introducing these Taylor expansions into the upwind scheme (38) leads to

$$\psi_i^n + \delta t \frac{\partial \psi}{\partial t} + \frac{1}{2} \delta t^2 \frac{\partial^2 \psi}{\partial t^2} = \psi_i^n - \frac{\delta t \, v}{\delta x} \left[\delta x \frac{\partial \psi}{\partial x} - \frac{1}{2} \delta x^2 \frac{\partial^2 \psi}{\partial x^2} \right] \tag{41}$$

We can eliminate the second derivative in time by using the PDE (36):

$$\frac{\partial^2 \psi}{\partial t^2} \stackrel{(36)}{=} -v \frac{\partial^2 \psi}{\partial t \partial x} \stackrel{(36)}{=} v^2 \frac{\partial^2 \psi}{\partial x^2} \tag{42}$$

Using this in (41) and rearranging the terms leads to the following equation

$$\frac{\partial \psi}{\partial t} = -\frac{\partial}{\partial x}(v\,\psi) - \frac{\partial}{\partial x} \left[-\frac{v\,\delta x}{2} \frac{\partial \psi}{\partial x} + \frac{v\,\delta t}{2} \frac{\partial}{\partial x}(v\,\psi) \right]. \tag{43}$$

We can interpret the last term in the square brackets for $\psi \neq 0$ as an anti-diffusive flux. This can be illustrated by defining an anti-diffusive pseudo-velocity $v_{\rm ad}$ which allows to write the equations which MPDATA solves as

$$\frac{\partial \psi}{\partial t} = -\frac{\partial}{\partial x} (v \,\psi) - \frac{\partial}{\partial x} (v_{\rm ad} \,\psi). \tag{44}$$

$$v_{\rm ad} = -\frac{v \, \delta x}{2\psi} \frac{\partial \psi}{\partial x} + \frac{v \, \delta t}{2\psi} \frac{\partial}{\partial x} (v \, \psi). \tag{45}$$

For the details of multidimensional definition of antidiffusive velocity, please refer to [4].

3.3.3.2 **Limiters for antidiffusive fluxes** The discussion on the FCT option of MPDATA can be found in section 3.2 of [3]. It begins with the search for the limiters (spatial indices were dropped for convenience):

$$\psi^{MAX} = max\left(\psi^{ant}, \psi^{ant}_{neighbours}, max(\psi^{in}, \psi^{in}_{neighbours})\right)$$
(46)

where ψ^{ant} is the first order approximation of ψ at time n+1 (after the first upwind pass) and ψ^{in} is the tracer field that enters the MPDATA procedure. The subscript $_{neighbours}$ describes set of values of ψ at the total of 6 nearest neighbouring points on A grid, that is i+1, j, k, i, j+1, k and so on. Next, limiting ratios are evaluated such that:

$$cp = \frac{\psi^{MAX} - \psi^{ant}}{\sum_{I=1}^{3} \left(-min(0, v_{I, left}^{ad}) + max(0, v_{I, right}^{ad})\right) + ep}$$

$$(47)$$

$$cp = \frac{\nabla}{\sum_{I=1}^{3} \left(-min(0, v_{I,left}^{ad}) + max(0, v_{I,right}^{ad})\right) + ep}$$

$$cn = \frac{\psi^{ant} - \psi^{MIN}}{\sum_{I=1}^{3} \left(max(0, v_{I,left}^{ad}) - min(0, v_{I,right}^{ad})\right) + ep}$$
(48)

Generalisation for the Sphere The unstructured MPDATA dwarf solves the following more general equation

$$\frac{\partial(G\,\psi)}{\partial t} + \frac{\partial}{\partial x}(v\,\psi) = 0,\tag{49}$$

where the symbol G describes geometric and physical terms (Jacobian of coordinate transformations and fluid density). We use in this dwarf the so called infinite-gauge version of MPDATA which allows the field ψ to change its sign by essentially removing ψ from the denominator in (45). This gives us together with the introduction of G the following expression for the pseudo-velocity $v_{\rm ad}$:

$$dv_{\rm ad} = -\frac{1}{2}|v|\frac{\partial\psi}{\partial x}\delta x + \frac{1}{2}u\,\delta t\left[\frac{\partial}{\partial x}(v\,\psi) + \psi\,\frac{\partial G}{\partial t}\right]. \tag{50}$$

Discretising (44) with forward difference in time gives

$$\psi_i^{n+1} = \psi_i^n - \delta t \frac{\partial}{\partial x} (v \, \psi) - \delta t \frac{\partial}{\partial x} (v_{\text{ad}} \, \psi). \tag{51}$$

The spatial derivatives are discretised with upwind fluxes which results in three dimensions in a sum of the upwind fluxes over all interfaces between neighbouring grid cells. The derivation of the multidimensional case and more details about its implementation are described in [2]. A pre-print of this paper can be found in doc/MPDATA-JCP2016.pdf in the git-repo.

Implementation The actual MPDATA algorithm is compactly coded in the *mpdatadwarf.F and *mpdatadwarf sphere.F90 files. The code is organised around main stencil computations, whereas the formulation of boundary conditions is hidden in auxiliary routines that perform simple operations (copy, negation, zero) on the outer

computational halo. MPI halo updates are performed by *update** routines that ultimately point to single halo update subroutine in **mpi_parallel.F90*.

The following pseudo-code exposes main stencil computations, while dismissing boundary conditions and halo updates that have minor effect on performance on typical number of cores. Typically, the algorithm is memory bound, so the motivation is to inform about the data access pattern characteristic to subsequent components of the MPDATA algorithm, as well as the range of computations sharing a single set of loops. The example given considers gauge version of MPDATA for cartesian domain, the spherical and standard MPDATA bear similar structure.

main program driver: loop over all timesteps. In each step (loops over i,j,k dropped for compactness):

Evaluate upwind algorithm (i.e. fully 3D first order forward-in-time advection algorithm: Here, x_in is the tracer input, xant is an auxiliary variable corresponding to the tracer after first upwind pass, rhr is the ratio of densities from the two subsequent timesteps (here equal unity, but preserved for exact reproduction of weather solver memory bandwidth requirements), hi is the inverse of density. Note that donor statement computes net flux through given finite volume boundary located at C-grid (where u1,u2 and u3 are defined). This step refers to term $-\frac{\partial}{\partial x}(v\psi)$ of the eq. 44.

```
\begin{array}{l} !\, donor\, (y1\,,y2\,,a) \,=\, max\, (0\,.\,,a) * y1\, -\, (-min\, (0\,.\,,a) * y2\,) \\ f1\, ij\, k\, p = donor\, (x_{\_}in\, (i\,\,.\,j\,\,,k)\,\,, x_{\_}in\, (i\,\,+1\,,j\,\,,k)\,\,, u1\, (i\,\,+1\,,j\,\,,k\,\,\,)) \\ f1\, ij\, k\, = donor\, (x_{\_}in\, (i\,\,-1\,,j\,\,,k)\,\,, x_{\_}in\, (i\,\,,j\,\,,k)\,\,, u1\, (i\,\,,j\,\,,k\,\,\,)) \\ f2\, ij\, k\, p = donor\, (x_{\_}in\, (i\,\,,j\,\,,k)\,\,, x_{\_}in\, (i\,\,,j\,+1\,,k)\,\,, u2\, (i\,\,,j\,+1\,,k\,\,\,)) \\ f2\, ij\, k\, = \ldots\, ;\, f3\, ij\, k\, p = \ldots\, ;\, f3\, ij\, k\, = \ldots\, \\ xant\, (i\,\,,j\,\,,k) = rhr\, (i\,\,,j\,\,,k) * \\ (x_{\_}in\, (i\,\,,j\,\,,k) - \\ (f1\, ij\, k\, p - f1\, ij\, k\,\, + f2\, ij\, k\,\, p - f2\, ij\, k\,\, + f3\, ij\, k\,\, p - f3\, ij\, k\,\, ) *\, hi\, (i\,\,,j\,\,,k)) \end{array}
```

Evaluate antidiffusive velocities v1,v2,v3: These are pseudovelocities that will be used in the second upwind iteration that corrects the excessive diffusion of the first-order upwind scheme. This is the most complex and computationally demanding component of MPDATA scheme. Formula for v1 is given below, whereas the formulas for v2 and v3 are very similar, only with permuted indices and transporting momenta components u1,u2,u3. Here h denotes the density. This step refers to evaluation of v_{ad} in the term $-\frac{\partial}{\partial x}(v_{ad}\psi)$ of the eq. 44.

```
\begin{array}{ll} ! & vdyf(x1,x2,a,rinv) = (abs(a) - a **2 * rinv) * rat2(x1,x2) \\ ! & rat4(z0,z1,z2,z3) = (z3 + z2 - z1 - z0) *.25 \\ \\ hmx = & 1./(0.5 * (h(i-1,j,k) + h(i,j,k))) \\ v1(i,j,k) = vdyf(xant(i-1,j,k),xant(i,j,k),u1(i,j,k),hmx) \\ & -0.125 * u1(i,j,k) * hmx* \end{array}
```

```
 ((u2(i-1,j-k)+u2(i-1,j+1,k)\\ +u2(i-1,j+1,k)+u2(i-1,j-1,k),\\ *rat4(xant(i-1,j-1,k),xant(i-1,j-1,k),\\ xant(i-1,j+1,k),xant(i-1,j-1,k))\\ +\\ (u3(i-1,j,k-1)+u3(i-1,j,k+1)\\ +u3(i-1,j,k+1)+u3(i-1,j,k+1)\\ *rat4(xant(i-1,j,k-1),xant(i-1,j,k-1),\\ xant(i-1,j,k+1),xant(i-1,j,k+1)))\\ ...\\ v2(i,j,k)=vdyf(xant(i,j-1,k),xant(i,j,k),u2(i,j,k),hmy)\\ ...\\ v3(i,j,k)=vdyf(xant(i,j,k-1),xant(i,j,k),u3(i,j,k),hmz)
```

Evaluate local maxima/minima of given tracer for limiters: The max/min operation is taken for in-place and neighbours in main directions, for subsequent use in flux limiting. Note that these are evaluated for timestep n and the first order approximation of tracer field at n+1. This is the implementation of the eq. 46.

Evaluate limiting members for flux-corrected transport: Note that small number ep is introduced to avoid division by zero. This is the implementation of the eq. 47.

```
\begin{array}{l} ! \, pp = \, \max \left( \, 0 \, . \, , \, y \right) \\ ! \, pn = - \min \left( \, 0 \, . \, , \, y \right) \\ cp \left( \, i \, , \, j \, , \, k \right) = \left( \max j k - \operatorname{xant} \left( \, i \, , \, j \, , \, k \right) \right) * h \left( \, i \, , \, j \, , \, k \right) / \\ \left( pn \left( v1 \left( \, i \, + 1 \, , \, j \, & \, k \, \right) \right) + pp \left( v1 \left( \, i \, , \, j \, , \, k \right) \right) \\ + pn \left( v2 \left( \, i \, & \, , \, j \, + 1 \, , \, k \, & \, \right) \right) + pp \left( v2 \left( \, i \, , \, j \, , \, k \right) \right) \\ + pn \left( v3 \left( \, i \, & \, , \, j \, & \, , \, k \, + 1 \right) \right) + pp \left( v3 \left( \, i \, , \, j \, , \, k \right) \right) + ep \right) \\ cn \left( \, i \, , \, j \, , \, k \right) = \left( \operatorname{xant} \left( \, i \, , \, j \, , \, k \, + 1 \right) \right) + pn \left( v1 \left( \, i \, , \, j \, , \, k \right) \right) \\ + pp \left( v2 \left( \, i \, & \, , \, j \, + 1 \, , \, k \, & \, \right) \right) + pn \left( v2 \left( \, i \, , \, j \, , \, k \right) \right) \\ + pp \left( v3 \left( \, i \, & \, , \, j \, & \, , \, k \, + 1 \right) \right) + pn \left( v3 \left( \, i \, , \, j \, , \, k \right) \right) + ep \right) \end{array}
```

Evaluate corrective upwind iteration: Here second upwind pass is applied, effectively acting as negative diffusion. The result is passed to the input/output

variable x_in . This step alludes to the evaluation of the term $-\frac{\partial}{\partial x}(v_{ad}\psi)$ of the eq. 44.

```
f1ijk =
                   ))*min(1.,cp( ,j,k),cn(i-1,j,k))
      pp(v1(i,j,k
     -pn(v1(i,j,k))*min(1.,cp(i-1,j,k),cn(i,j,k))
f1ijkp =
      pp(v1(i+1,j,k))*min(1.,cp(i+1,j,k),cn(i-1))
     -pn(v1(i+1,j,k))*min(1.,cp(i,j,k),cn(i+1,j,k))
f2ijk =
      pp(v2(i,j,k))*min(1.,cp(i,j,k),cn(i,j-1,k))
     -pn(v2(i,j,k))*min(1.,cp(i,j-1,k),cn(i,j,k))
f2ijkp = \dots
f3ijk = \dots
f3ijkp = \dots
x_{in}(i, j, k) = (xant(i, j, k) / rhr(i, j, k) -
                         (flijkp-flijk
                          +f2ijkp-f2ijk
                          +f3ijkp-f3ijk) * hi(i,j,k))
```

3.3.4 Dwarf usage and testing

In this section we describe how to download and install the dwarf along with all its dependencies, and we show how to run it for a simple test case.

Note that the MPDATA dwarf for structured meshes has no external dependences. Therefore, besides the generic ESCAPE build strategy it allows for manual build with Makefile, respective Makefiles are provided in *manualbuild** directories. The dwarf is written in Fortran 95/2003.

3.3.4.1 Download and installation The first step is to download and install the dwarf along with all its dependencies. With this purpose, it is possible to use the script provided under the ESCAPE software collaboration platform: https://git.ecmwf.int/projects/ESCAPE.

Here you can find a repository called <code>escape</code>. You need to download it. There are two options to do this. One option is to use ssh. For this option you need to add an ssh key to your bitbucket account at https://git.ecmwf.int/plugins/servlet/ssh/account/keys. The link "SSH keys" on this website gives you instructions on how to generate the ssh key and add them to your account. Once this is done you should first create a folder named, for instance, ESCAPE, enter into it and subsequently download the repository by using the following the steps below:

```
mkdir ESCAPE
cd ESCAPE/
git clone ssh://git@git.ecmwf.int/escape/escape.git
```

The other option to download the repo is by using https instead of ssh. Instead of the git command above you then need to use

```
git clone https://<username>@git.ecmwf.int/scm/escape/escape.git
```

where <username> needs to be replace by your bitbucket username.

Once the repository is downloaded into the ESCAPE folder just created, you should find a new folder called <code>escape</code>. The folder contains a sub-folder called <code>bin</code> that has the python/bash script (called <code>escape</code>) that needs to be run for downloading and installing the dwarf and its dependencies. To see the various options provided by the script you can type:

```
./escape/bin/escape -h
```

To download the dwarf you need to run the following command:

```
./escape/bin/escape checkout dwarf-D-advection-MPDATA-structured \
--ssh
```

To use https you need to replace —ssh with —user <username>. The commands above automatically check out the **develop** version of the dwarf. If you want to download a specific branch of this dwarf, you can do so by typing:

```
./escape/bin/escape checkout dwarf-D-advection-MPDATA-structured --user <username> --version <br/> transfer of the control of
```

You should now have a folder called dwarf-D-advection-MPDATA-structured.

In the above command, you can specify several other optional parameters. To see all these options and how to use them you can type the following command:

```
./escape checkout -h
```

At this stage it is possible to install the dwarf and all its dependencies. This can be done in two different ways. The first way is to compile and install each dependency and the dwarf separately:

```
./escape/bin/escape generate-install dwarf-D-advection-MPDATA-structured
```

The command above will generate a script called install-dwarf-D-advection-MPDATA that can be run by typing:

```
./install-dwarf-D-advection-MPDATA-structured
```

This last step will build and install the dwarf along with all its dependencies in the following paths:

```
dwarf-D-advection-MPDATA-structured/builds/
dwarf-D-advection-MPDATA-structured/install/
```

The second way is to create a bundle that compiles and installs all the dependencies together:

```
./escape/bin/escape generate-bundle dwarf-D-advection-MPDATA-structured
```

This command will create an infrastructure to avoid compiling the single third-party libraries individually when some modifications are applied locally to one of them. To complete the compilation and installation process, after having run the above command for the bundle, simply follow the instructions on the terminal.

In the commands above that generate the installation file, you can specify several other optional parameters. To see all these options and how to use them you can type the following command:

```
./escape generate-install -h
./escape generate-bundle -h
```

3.3.4.2 Manual building This dwarf has no external dependencies, so the build process can be easily controlled by hand. For this purpose, makefiles for each subdwarf are provided in the dwarf directory in

```
./sources/dwarf-D-advection-MPDATA-structured/manualbuild-gauge
./sources/dwarf-D-advection-MPDATA-structured/manualbuild-standard
./sources/dwarf-D-advection-MPDATA-structured/manualbuild-sphere
```

The makefiles expose the preprocessor definitions mentioned above and contain a set of bit reproducible, standard and advanced optimisation options for Cray, NAG, PGI, Intel and GNU compilers. For porting of the makefile on given machine it should be sufficient to properly point FTN_NOMPI and FTN_MPI variables to the actual system commands invoking Fortran compilers in serial and parallel configuration.

3.3.4.3 Testing Contrary to unstructured advection dwarf, the testing is implemented within the dwarf binary itself. The MPDATA gauge and MPDATA gauge-sphere subdwarfs provide measure of L2 "energy" conservation error norm, for the reference configurations of 59^3 cubic cartesian box (discussed recently in section 3.7 in [1], and 128x64xL lon-lat-L spherical grid, originally defined in [5] and recently referred to in section 3.8 of [1]. The cartesian test represents three-dimensional sphere revolving around tilted axis with constant angular velocity; the error is measured exactly after one revolution. Standard MPDATA subdwarf is not provided with the reference solution as the reference results were not published for this particular setup, although the L2 error is computed as in the gauge subdwarf. In turn, the spherical test bases on the 2D solid-body rotation on a spherical

surface. The trajectory of solid-body is set so it starts from the equator (where the grid is the relatively coarse) and it travels along meridian towards the pole, where the grid spacing in longitudinal direction is minimal. For each subdwarf, evaluation of the error norms at the end of integration can be deactived using TESTING definition in cmake script.

The dwarfs also employs custom execution timers for the actual dwarf subroutine and halo update routines (metrics are inclusive). The table appearing at the of integration provides information on number of calls to a particular routine, average timer on all cores along with maximum and minimum time of execution for given MPI process. This measurement should be used when comparing different computer architectures. For accelerators please also include a measurement that includes the process of copying the data to the device. Please report your measurements (no matter if they are good or bad) on https://confluence.ecmwf.int/display/ESCAPE/Dwarf+-+D+-+advection+-+MPDATA+-+structured by following the example under the section "Performance Measurements" of that website. This feature can be switched off with the TIMERSCPU definition in cmake file.

The dwarf allows for testing with static and dynamic memory allocation. This reveals the added value of the predefined size of matrices and loops at compile time. Static memory allocation can be controlled with STATICMEM define in cmake script.

3.3.5 Run the Dwarf

If you want to run the dwarf in your local machine, you could do so by using the executable subdwarf files inside

```
dwarf-D-advection-MPDATA-structured/install/\
dwarf-D-advection-MPDATA-structured/bin/
```

If you instead want to run the dwarf on an HPC machine available to the ESCAPE partners, you can automatically generate the job submission script with the **escape** file.

More specifically, the following command (example for gauge subdwarf):

```
./escape generate-run -c \
"dwarf-D-advection-MPDATA-structured/install/\
dwarf-D-advection-MPDATA-structured/bin/\
dwarf_D_advection_MPDATA_structured_gauge"
```

allows the code to generate the submission script for the given HPC machine you are targeting without submitting the actual job. The command above will in fact simply generate an <code>escape.job</code> file in the current folder. This can successively be submitted via <code>qsub</code> on the HPC machine you want to run the simulation on.

In the above command you can specify several other optional parameters, such as wall-time, number of tasks, number of threads, etc. To see all these options and how to set them up you can type the following command:

./escape generate-run -h

Warning



However, note that for execution on more than one core you need to manually modify the *parameters*.F90 file for the given subdwarf, where parameters nprocx, nprocy, nprocz are defined. Given dwarf must be then recompiled, as for the static memory allocation the size of MPI subdomain implicates the allocation of matrices performed at compile time.

The following subsections describe how the precision of the computation can be selected and the data generated by the simulation in the log- and output-files.

3.3.5.1 Switching between single and double precision The dwarf has been tested with single as well as double precision. To switch between single and double precision please adjust the line INTEGER, PARAMETER:: euwp = sp inside the file dwarf_D_advection_MPDATA_structured_precisions.F90. Setting euwp = dp in this line uses double precision for the entire simulation whereas euwp = sp uses single precision.

3.3.6 References for structured MPDATA

- [1] A. Jaruga et al. "libmpdata++ 1.0: a library of parallel MPDATA solvers for systems of generalised transport equations". In: Geoscientific Model Development 8.4 (2015), pp. 1005–1032. DOI: 10.5194/gmd-8-1005-2015. URL: https://www.geoscimodel-dev.net/8/1005/2015/.
- [2] C. Kühnlein and P.K. Smolarkiewicz. "An unstructured-mesh finite-volume MP-DATA for compressibleatmospheric dynamics". In: *Journal of Computational Physics* (submitted 2016).
- [3] Piotr K Smolarkiewicz and Wojciech W Grabowski. "The multidimensional positive definite advection transport algorithm: Nonoscillatory option". In: *Journal of Computational Physics* 86.2 (1990), pp. 355–375.
- [4] Piotr K. Smolarkiewicz and Len G. Margolin. "MPDATA: A Finite-Difference Solver for Geophysical Flows". In: *Journal of Computational Physics* 140.2 (1998), pp. 459–480. ISSN: 0021-9991. DOI: https://doi.org/10.1006/jcph.1998.5901. URL: http://www.sciencedirect.com/science/article/pii/S0021999198959010.
- [5] Piotr K Smolarkiewicz and Philip J Rasch. "Monotone advection on the sphere: An Eulerian versus semi-Lagrangian approach". In: *Journal of the Atmospheric Sciences* 48.6 (1991), pp. 793–810.

3.4 ACRANEB2 radiation scheme

3.4.1 Scope

The radiation schemes in numerical weather prediction and climate models take up a considerable amount of the overall running time of these models. Here, "radiation" is implicitly taken to mean *electromagnetic radiation*. The heating due to absorption of shortwave (solar) and longwave (terrestrial heat) radiation is the initial driver of all atmospheric processes with the exception of volcanic events.

Neither the shortwave nor the longwave radiative transfer can be solved within a reasonable amount of time from basic principles. In addition to the spatial and temporal approximations that are necessary to make for all physical processes in atmospheric models, it is necessary to make approximations in the spectral dimension and the directional dimensions. Thus, it is not feasible to calculate the radiative transfer for each absorbing and emitting line of the atmospheric gasses; in stead a limited number of spectral bands are defined for which the radiative transfer is calculated. For shortwave irradiance the radiative transfer in most current models is only considered for the direct solar beam, upward diffuse irradiance and downward diffuse irradiance. Thus, the complex directional variability of shortwave irradiances is not considered. This is called the two-stream approximation. For the longwave irradiances the two-stream approximation is also used in most current models. To sum up, many approximations are currently made in order to calculate radiative transfer in weather and climate models, and yet these are very resource demanding. A better utilisation of the radiation schemes on current and future extremely parallelised multi-threaded CPUs and GPUs is in demand.

Given these many ways radiation schemes can be approximated, they can be, and have been, designed in various ways. For radiation schemes in medium to long range weather models, it makes sense to utilise more spectral bands to capture the complex shortwave radiative heating in the stratosphere while saving resources in the spatial and temporal dimensions by running the radiation scheme in coarser resolution and intermittently relative to the general model time stepping. For radiation schemes in short range convective permitting weather models, on the other hand, it makes sense to resolve the diabatic heating patterns caused by small scale clouds, and not to use resources to improve the accuracy of the stratospheric heating rates. Here we have chosen to work with the ACRANEB2 radiation scheme [1, 3], which is made for short range weather models. This dwarf has many of the features of physics modules in weather and climate models in general. Thus, it includes frequent usage of transcendental functions, and complex loop and conditional structures. This makes it interesting also in a broader context.

The overarching scope of this dwarf can be summarised in the following questions:

- 1. What is the potential of refactoring the dwarf to run optimally on 2016 model Xeon, Xeon Phi processors and GPUs?
- 2. Is it worthwhile refactoring a physics subroutine such as this?

- 3. Should the refactoring be done universally for the different hardware architectures investigated?
- 4. Can a set of rules be made for proper programming optimised for current hardware architectures?

Detailed descriptions of the physics in ACRANEB2 have been made by Mašek et al. (2016) [1] and Geleyn et al. (2017) [3] for the shortwave and longwave radiation, respectively. The work package 2 (WP2) software adaptation of the ACRANEB2 dwarf, and the benchmarking and diagnostics results for different hardware architectures (WP3) are detailed in the report by Poulsen and Berg (2017) [2]. In this WP1 deliverable the focus is on how the original radiation scheme subroutines have been adapted to become a dwarf, and the subsequent dwarf versions developed from the initial version. How the dwarf should be run and can be modified is also described.

3.4.2 Objectives

The main objective of this deliverable is to port the underlying code to accelerator and multithreaded architecture environments, and to document how the dwarf is run. The dwarf is then ready to be software-refactored (WP2) and tested on selected hardware architectures (WP3).

The objectives are:

- to make a stand-alone dwarf version of ACRANEB2 for different hardware architectures,
- to make dwarfs of particularly computationally intensive parts of ACRANEB2 if needed,
- to check the reproducibility of the dwarf output for given input for different compilers and compiler options,
- to measure the time-to-solution provided by implementations of the spectral transform on different hardwares, and
- to make a method for assessing the energy-to-solution.

To achieve these goals we have made two prototypes of the ACRANEB2 dwarf. The first prototype <code>dwarf-lonlev-0.24</code> is a stand-alone version that can be run with given input data, namelist input, and which provides output as the original subroutine. Relative to the original version of the subroutine, the loop structure has been changed so that loops over model levels are the innermost loops, rather than the outermost loops. Timing statements have also been added and other minimal changes to ensure portability have been made. The second prototype <code>dwarf-lonlev-0.9</code> has been optimised for running on 2016 model Xeon Phi processors as documented by Poulsen and Berg (2017) [2].

Furthermore, three prototypes based on a particularly computationally intensive part of ACRANEB2—the 'transt3' dwarf—have been made. The first of these dwarf-transt3_v0.1 has been optimised for running on 2016 model Xeon Phi processors. The second two of these dwarf-transt3_gpu_v0.2 and dwarf-transt3_gpu_nproma_v0.1 have been optimised for running on 2016 model GPUs. Here, the third transt3 version has loops that are tailor-made for the specific GPU tested.

3.4.3 Description of Dwarf prototypes

The Dwarf-P-ACRABNEB2-radiation scheme calculates atmospheric heating rates and specific downward surface fluxes for both shortwave and longwave radiation. To make a stand-alone version that can be run and tested as a dwarf, we have made a simple Fortran program structure that reads input from namelist files and modules, and writes formatted and binary output. As mentioned in section 3.4.2 we have two prototypes of the ACRANEB2 dwarf. After installing the dwarf with the escape script as described above these prototypes can be found in the respective folders

```
escape-acraneb2-dwarf/src/dwarf-lonlev-0.24 and escape-acraneb2-dwarf/src/dwarf-lonlev-0.9.
```

In the following subsections these folders will be referred to with the generic name <dwarf>/.

3.4.3.1 Namelist input variables Namelists make it possible to run different experiments without having to recompile the code. We have made two namelists

```
escape-acraneb2-dwarf/test/escape-acraneb2-input/dimensions.nam and escape-acraneb2-dwarf/test/escape-acraneb2-input/nam radia dwarf.nam.
```

In dimensions.nam the spatial dimensions of the input data for the dwarf are specified as the number of longitudes KLO, latitudes KLA and levels KLEV for the rectangular model grid. As is the case with most weather and climate model subroutines, the three dimensional space is reduced to two dimensions KLON and KLEV, where the former is the total number of horizontal elements, that is the product of KLO and KLA. This is done since the radiative (and other physical) processes are calculated as occurring in independent columns in the model grid. By default KLON = 160000 or 400 by 400 and KLEV = 80.

In the namelist nam_radia_dwarf.nam several variables are defined from which input data for the acraneb2 subroutine can be calculated. The point of this setup is to be able to easily make realistic input data without having to specify this for each grid box. Some of the variables in nam_radia_dwarf.nam are unused in the default version, but could be utilised as desired.

The atmospheric model level input variables needed by the acraneb2 subroutine are temperature (T), specific humidity (q), cloud cover ("NEB"), ice cloud load ("ICE"), liquid cloud load ("LI"), aerosol profiles (6 types), gasses (important for radiation), half level, full level pressures and pressure thicknesses. Additionally, the surface variables

needed are diffuse and direct albedo, emittance and surface temperature. The full acraneb2 input is calculated in the subroutines <dwarf>/src/ini_var_ideal.F90 and <dwarf>/src/ini acraneb.F90.

In nam_radia_dwarf.nam variables that reflect the namelist variables that control how ACRANEB2 is run in both the full ALARO-1 and HARMONIE-AROME NWP models can be found. These are listed below.

- LRNUMX is a logical variable that chooses maximum-random cloud overlap. If the variable is set to false, random cloud overlap is chosen. For this version of ACRANEB2, it is recommended to be set to true.
- LCLSATUR is a logical variable that makes the cloud optical coefficients depend on the liquid/ice water content, and the saturation effect depend on cloud layers above and below. This should be set to true.
- LVOIGT and LVFULL are logical variables that accounts for the effect of Doppler line broadening in the mesosphere [1], which results in the Voigt line shape. For short range forecasting models with the highest model levels in the stratosphere, this effect can be ignored. These variables are set to true by default.
- LRAYLU is a logical variable that activates computation of lunar surface fluxes. This variable is set to false.
- LRPROX is a logical variable that switches on exact adjacent exchanges of thermal irradiances. This should be switched off to get a better inclusion of cloudiness (pers. comm. Mašek 2013) and is therefore set to false.
- LRTPP is a logical variable that switches on nonisothermal layer correction in adjacent exchanges. This is set to true by default.
- LRAYPL is a logical variable that accounts for using a shorter horizontal array for shortwave computations when the model domain is only partially daylit. This option has been removed in the refactored dwarf-lonlev-0.9.
- NPHYREP is an integer variable for code tests. For this dwarf it should always be set to 1.
- NSORAYFR is an integer variable that controls the intermittency of the full solar radiation computations. If it is 1, the full radiation is run at each time step, if is 2 it is run at every other time step, and so forth. If it is set to -1, the full radiation is run once every hour. For the original version of ACRANEB2 the default value is -1. For the refactored dwarf-lonlev-0.9 this option cannot be used and is thus always 1.
- NTHRAYFR is an integer variable that controls the intermittency of the full thermal radiation computations. If it is 1, the full radiation is run at each time step, if is 2 it is run at every other time step, and so forth. If it is set to -1, the full radiation is run once every hour. For the original version of ACRANEB2 the default value is -1. For the refactored dwarf-lonlev-0.9 this option cannot be used and is thus always 1.

- NRAUTOEV is an integer variable that controls the intermittency of the full computations of bracketing weights relative to the full computations of the thermal radiation. In the original version of ACRANEB2 the default value is 3 or every three hours. For the refactored dwarf-lonlev-0.9 this option cannot be used and is thus always 1.
- 3.4.3.2 Modules The original acraneb2 subroutine reads a large amount of natural constants and coefficients from module files. For the dwarf we have gathered all of these in one module <dwarf>/src/yomrad.mod with its variables being defined in the subroutine <dwarf>/src/ini_modules.f90. The module parkind.f90 is also used, which is a standard module defining variable types.

The module <dwarf>/src/dmi_timer.f90 has been developed by Jacob Weismann Poulsen and Per Berg (DMI) in order to ensure that timing estimates of the full dwarfs and their parts can be performed accurately and with a minimal amount of uncertainty. This is included in all dwarf prototypes. Calls to the timer subroutine from this module are added around the call to the acraneb2 subroutine itself, so that the overhead of the surrounding initialisation, input and output statements are not included in the time-to-solution computations.

- 3.4.3.3 Wrapping dwarf structure The wrapping structure to call and test the ACRANEB2 dwarf consists of the simple Fortran program <dwarf>/src/callmain.f90, which calls the subroutine <dwarf>/src/main.f90 from which the dimensions namelist and the subroutine <dwarf>/src/radia_dwarf.f90 are called. The subroutine <dwarf>/src/radia_dwarf.f90 contains the calls to the other module and initialisation subroutines described above, the calls to the input and output subroutines, and the call to <dwarf>/src/acraneb2.f90—the subroutine of primary interest.
- 3.4.3.4 The initial ACRANEB2 dwarf The initial prototype dwarf-lonlev-0.24 is modified relative to the original version of the subroutine: Minimal changes have been made in order to ensure portability, timing statements have been added, and the loop order has been changed so that the horizontal loops over model columns (JLON) are the outermost loops, while the loops over model levels (JLEV) are the innermost loops. The difference can be seen by comparing Fig. 1 and Fig. 2. Given that the total number of model columns in a typical limited area model is of the orders 10⁵–10⁶ and the number of model levels is of the order of 10², the largest loops are now on the outside. When the loops are switched, the size of the local variables can be reduced to single columns and scalars, which reduces the stack memory load. For the exascale weather and climate models of the future the relative differences in the JLON vs the JLEV loops will be even larger.

The subroutine acraneb2 includes comments that labels the sections of the code. In sections I and II, initialisations, aerosol optical properties and preliminary calculations are made. Of primary importance is here the computation of the variables ICALS and ICALT that control the intermittency of the shortwave and longwave radiation computations,

Figure 1 Example from the original subroutine acraneb_transt.f90 showing the original loop structure.

Figure 2 Example from the initial dwarf version of the subroutine acraneb_transt.f90 showing the revised loop structure. This is the same part of the subroutine as shown in Fig. 1. The JLON loop cannot be seen here, as this is now moved to include a larger part of of subroutine.

respectively. Here ICALS depends on the time step KSTEP and NSORAYFR, while ICALT depends on the KSTEP, NTHRAYFR and NRAUTOEV as explained in section 3.4.3.1. The default setup namelist nam_radia_dwarf.nam enables ICALS = 0 and ICALT = 2. In this part of the code the special case JLON loop indices IIDIA(IAUCR) and IFDIA(IAUCR) are also calculated. These define the columns that are sunlit, in cases where the model domain is only partially sunlit, and replace the standard JLON loop indices KIDIA and KFDIA.

Next the gaseous optical properties are calculated in section III. This includes calls to the subroutines $<dwarf>/src/acraneb_transs.f90$ and

<dwarf>/src/acraneb_transt.f90 in which the (descending and ascending) optical

depths in the shortwave and longwave spectral bands are calculated, respectively. The longwave gasseous optical depths are calculated both for the local temperatures and the temperature of the emitting body following the method of [4]. The subroutine acraneb_transs includes the subroutine delta_s_sca. This has been modified from the original version delta_s, where the added letters sca are short for scalar and reflect the dimensional reduction of the variables that was enabled by rearranging the overall loop structure of the acraneb2 subroutine. Likewise acraneb_transt includes calls to the subroutines delta_c_sca and delta_t_sca that are simplified versions of the original subroutines delta_c and delta_t.

After this, the cloud optical properties for the delta-two stream and adding radiative transfer computations are computed, mainly in the subroutine

<dwarf>/src/ac_cloud_model2.f90. In section IV of the code cloud overlap effects are
accounted for.

The longwave radiative transfer computations are performed in sections V-VIII. Here the subroutines <dwarf>/src/acraneb_coeft.f90,

<dwarf>/src/acraneb_solvt.f90 and <dwarf>/src/acraneb_solvt3.f90 are
called. In the former matrix coefficients for the adding method linear system are computed,
while this is solved by Gaussian elimination back-substitution in the two other subroutines.

The shortwave radiative transfer computations are performed in section IX. Here the subroutines <dwarf>/src/acraneb_coefs.f90 and

<dwarf>/src/acraneb_solvs.f90 are called. In the former matrix coefficients for the adding method linear system are computed, while this is solved by Gaussian elimination back-substitution in the latter.

3.4.3.5 The refactored ACRANEB2 dwarf

escape-acraneb2-dwarf/src/dwarf-lonlev-0.9 is refactored for the optimal time-to-solution performance on the Xeon Phi targets (KNL-7210 and KNL-7250). Regarding the overall structure, the main code has been gathered into the two modules acraneb2_m and <dwarf>/src/acraneb3.f90. Here the acraneb3 module contains all the subroutines that are called from the acraneb2 subroutine, while the acraneb_2m module contains the primary subroutine acraneb2 and the added subroutines acraneb2_heap and acraneb2_numainit. These two subroutines are called immediately before the acraneb2 call and ensure that the largest arrays are moved the memory heap and that these arrays are properly NUMA-initialised, respectively. Correspondingly, two calls are made to the subroutines radia_dwarf_heap and radia_dwarf_numainit from <dwarf>/src/main.f90 in the subroutine structure that surrounds the radiation routine (see section 3.4.3.3).

A detailed description of this dwarf prototype can be found in the report [2]. Here we will only add a summary of the steps taken in order to refactor the code:

- 1. Establish a solid reference (test case and source code) that reproduces the necessary results.
- 2. Establish build and run environment to ease repetition and reproducibility.

- 3. Ensure proper threading, i.e. a SPMD approach.
 - This requires a transition to Fortran90 assumed shape and trimming stack memory usage, and
 - contiguous data
- 4. Strive towards a minimal implementation, including:
 - Reducing the memory overhead.
 - Reducing the stack pressure by reducing local 2D/3D variables to 1D/2D vars or even scalars.
 - The largest stack arrays should be moved to the heap with proper NUMA initialisation of these heap arrays.
 - Collapsing loops over the outermost index.
 - Symbolic algebraic reduction using pen&paper.
 - Assuring no side effects in local functions (pure in Fortran).
 - Declaring constants as constants (parameter in Fortran), not as variables.
 - Moving all branching out of the loops.
- 5. Continued refactoring by shuffling computations around to maximize parallel exposure (playing with data structures and loops).
 - Identifying computational patterns, e.g. with reduction and prefix sums, and
 - ... without (SIMD-suitable loops) dependencies.
 - Re-organising heavy loops to constant trip-counts.

This list is taken from the presentation: "Performance studies (ACRANEB2)" by Per Berg and Jacob Weismann Poulsen given at the ESCAPE young scientist summer school in Copenhagen, August 2017. The full presentation is available from: http://www.hpc-escape.eu/media-hub/escape-events/ysss2017.

The module <dwarf>/src/dmi_omp.f90 has been added. From this the subroutine domp_get_domain is called in order to balance the thread load based on local properties of ACRANEB2 [2].

Of more basic structural changes a main thing is that the subroutine acraneb_transt has been divided into three seperate subroutines: acraneb_transt1,

acraneb_transt2 and acraneb_transt3, which primarily cover the computations of descending optical depths (1), ascending optical depths (2) and the intermediate optical depths for the thermal radiative exchange between layers (3). Of these acraneb_transt3 has been found to be the most time-consuming subroutine and therefore particular focus has been given to this in the refactoring process. In this the loop structure has been reduced to a triangular loop structure in the refactoring process [2]. The delta_c_sca and delta_t_sca subroutines within acraneb_transt have been rearraged in 6 differenct functions: zcdelta1, zcdelta2, zcdel0, ztdelta1, ztdelta2 and ztdel1. This done to remove conditional statements at this deeply nested level of the code.

Other structural changes include that the subroutine ac_cloud_model2_t now have replaced the ac_cloud_model2 subroutine. In the refactored version the number of output arrays is reduced, since these were only local arrays that could be calculated more efficiently at a later point in the code. The subroutines acraneb_coeftv0 and acraneb_coeftv1 replace the subroutine acraneb_coeft. With two subroutines replacing one subroutine conditional statements are again avoided.

3.4.3.6 Transt3 dwarfs for GPUs and Xeon Phi processors The dwarf version dwarf-transt3_v0.1 is a stand-alone version of the transt3 subroutine described above (section 3.4.3.5). Given that this subroutine takes more than 80% of the total running time of ACRANEB2 [2], it has been singled out for the optimised test on GPUs. This version is made for direct comparisons with the GPU-optimised dwarf versions dwarf-transt3_gpu_v0.2 and dwarf-transt3_gpu_nproma_v0.1. The "nproma" version of the GPU-optimised dwarf is hard-coded to run with NPROMA set to a length of 32, since this was found to be optimal for the P100 GPU that has been tested [2].

Binary input for these three dwarf versions are available in the file escape-acraneb2-dwarf/test/escape-acraneb2-input/transt_in.bin.

3.4.4 Dwarf installation and testing

The first step is to download and install the dwarf along with all its dependencies. With this purpose, it is possible to use the script provided under the ESCAPE software collaboration platform:

https://git.ecmwf.int/projects/ESCAPE.

Here you can find a repository called <code>escape</code>. You need to download it. There are two options to do this. One option is to use ssh. For this option you need to add an ssh key to your bitbucket account at https://git.ecmwf.int/plugins/servlet/ssh/account/keys. The link "SSH keys" on this website gives you instructions on how to generate the ssh key and add them to your account. Once this is done you should first create a folder named, for instance, ESCAPE, enter into it and subsequently download the repository by using the following the steps below:

```
mkdir ESCAPE
cd ESCAPE/
git clone ssh://git@git.ecmwf.int/escape/escape.git
```

The other option to download the repo is by using https instead of ssh. Instead of the git command above you then need to use

```
git clone https://<username>@git.ecmwf.int/scm/escape/escape.git
```

where <username> needs to be replace by your bitbucket username.

Once the repository is downloaded into the **ESCAPE** folder just created, you should find

a new folder called **escape**. The folder contains a sub-folder called **bin** that has the python/bash script (called **escape**) that needs to be run for downloading and installing the dwarf and its dependencies. To see the various options provided by the script you can type:

```
./escape/bin/escape -h
```

To download the dwarf you need to run the following command:

```
./escape/bin/escape checkout dwarf-P-radiation-ACRANEB2 \
--ssh
```

To use https you need to replace —ssh with —user <username>. The commands above automatically check out the **develop** version of the dwarf. If you want to download a specific branch of this dwarf, you can do so by typing:

```
./escape/bin/escape checkout dwarf-P-radiation-ACRANEB2 --user <username> \
--version <branch-name>
```

You should now have a folder called dwarf-P-radiation-ACRANEB2 with all 5 dwarf prototypes mentioned above inside of

dwarf-P-radiation-ACRANEB2/sources/dwarf-P-radiation-ACRANEB2/src. Each of these can then be configured and compiled with standard configure and make commands. Examples are given in the scripts <dwarf>/confmake.sh for each of the dwarf versions. See also the README file: README-escape-acraneb2-dwarf.txt.

3.4.5 Running the Dwarf

The ACRANEB2 prototypes are configured and made with the confmake.sh script. On the KNL cluster cck at ECMWF you must first swap to the Intel environment:

```
module swap PrgEnv-cray PrgEnv-intel
```

You can now use

```
cd <dwarf_directory>
./confmake.sh
```

and submit the dwarf to the queue with:

```
qsub submit.sh
```

To run the dwarf prototypes optimised for GPU processors on the GPU cluster lxg at ECMWF (K80 NVIDIA GPUs) you must first load and swap the modules:

```
module load cuda
```

```
module load openmpi
module swap gnu pgi
```

Then run:

```
cd <dwarf_directory>
./confmake.sh
```

and submit the dwarf with:

```
sbatch submit_gpu.sh
```

3.4.6 Conclusion remarks

As this deliverable is being written, much work has already been done on the software adaptation (WP2) and benchmarking and diagnostics (WP3) for the ACRANEB2 dwarf. Based on this work, the following answers can be given to the questions posed in section 3.4.1:

- 1. The potential of refactoring ACRANEB2 to run optimally contemporary Xeon, Xeon Phi processors and GPUs is very large.
- 2. We find it very likely that this is the case for legacy physics routines used in weather and climate models in general.
- 3. For a complex physics subroutine, such as this, we found that different refactoring was needed for the GPUs and the Xeon Phi processors.
- 4. Rules can be made for how to adjust legacy physics code for optimised running on current hardware architectures, however, the work of specialists is required! Such an investment is worthwhile given the significant improvement in time-to-solution and reduction in energy consumption that can be achieved.

3.4.7 References for ACRANEB2

- [1] J. Mašek et al. "Single interval shortwave radiation scheme with parameterized optical saturation and spectral overlaps". In: Q. J. R. Met. Soc. 142.694 (2016), pp. 304–326. DOI: 10.1002/qj.2653.
- [2] J. W. Poulsen and P. Berg. Tuning the implementation of the radiation scheme ACRANEB2. Tech. rep. 17-22. Danish Meteorological Institute, Copenhagen, Denmark, 2017.
- [3] J.-F. Geleyn et al. "Single interval longwave radiation scheme based on the net exchanged rate decomposition with bracketing". In: Q. J. R. Met. Soc. 143.704 (2017), pp. 1313–1335. DOI: 10.1002/qj.3006.

[4] V. Ramanathan and P. Downey. "A nonisothermal emissivity and absorptivity formulation for water vapor". In: *J. Geophys. Res.* 91.D8 (1986), pp. 8649–8666. DOI: 10.1029/JD091iD08p08649.

4 Conclusions

A second set of weather and climate prediction model sub-components (dwarfs) has been established, documented and made available for uptake and testing by the ESCAPE project partners. These new dwarfs extend the range of computational characteristics in terms of memory bandwidth, communication and computational cost. The new multigrid preconditioned elliptic solver poses new challenges in terms of next neighbour communication. The two MPDATA dwarfs allow an interesting insight into comparing the optimisation potential of structured and unstructured meshes. The radiation dwarf represents a very important part of the physics computation and forms together with the cloud microphysics dwarf from the first batch the second dwarf in the physics category.

The completion of this deliverable allows to progress with subsequent tasks of ESCAPE dealing with code adaptation and performance evaluation on the available hardware architectures. The work on porting these new dwarfs to GPUs and Xeon Phi processors as well as using domain specific languages has started in working packages 2 and 3. First results have been reported in D3.3.

The deliverable has been produced on time and its outcome has been disseminated to project partners through the proposed mechanisms of ESCAPE.

Document History

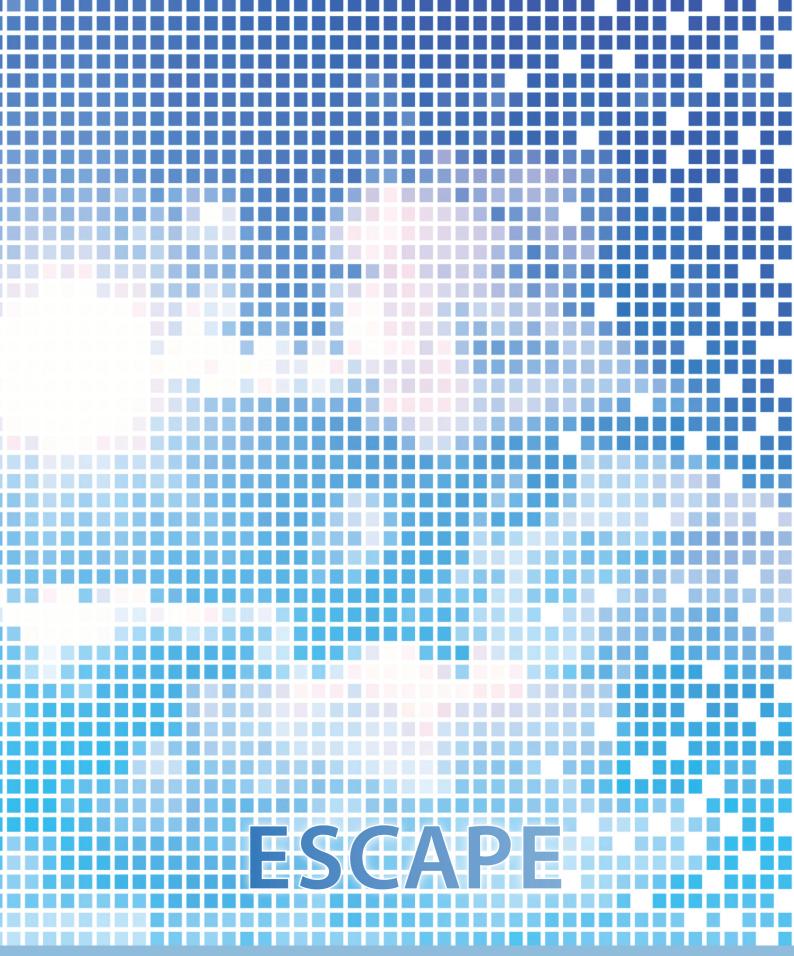
Version	Author(s)	Date	Changes
0.1	Andreas Mueller	04/12/2017	First Draft
0.2	Andreas Mueller	06/12/2017	Added contribution from PSNC
0.3	Andreas Mueller	08/12/2017	Version for internal review
1.0	Andreas Mueller	19/12/2017	Final version
1.1	Andreas Mueller	18/01/2019	Git-repo addresses updated

Internal Review History

Internal Reviewers	Date	Comments
Philippe Marguinaud, Michael Glinton	18/12/2017	Approved with Comments
Michal Kulczewski	15/12/2017	Approved with Comments

Effort Contributions per Partner

Partner	Efforts
ECMWF	8
LU	1
PSNC	3
DMI	4.8
Total	16.8



ECMWF Shinfield Park Reading RG2 9AX UK Contact: peter.bauer@ecmwf.int

The statements in this report only express the views of the authors and the European Commission is not responsible for any use that may be made of the information it contains.